Spontaneous Channel Activity of the Inositol 1,4,5-Trisphosphate ($InsP_3$) Receptor ($InsP_3R$). Application of Allosteric Modeling to Calcium and $InsP_3$ Regulation of $InsP_3R$ Single-channel Gating

Don-On Daniel Mak, Sean M.J. McBride, and J. Kevin Foskett

Department of Physiology, University of Pennsylvania, Philadelphia, PA 19104

ABSTRACT The $InsP_3R$ Ca^{2+} release channel has a biphasic dependence on cytoplasmic free Ca^{2+} concentration ($[Ca^{2+}]_i$). $InsP_3$ activates gating primarily by reducing the sensitivity of the channel to inhibition by high $[Ca^{2+}]_i$. To determine if relieving Ca^{2+} inhibition is sufficient for channel activation, we examined single-channel activities in low $[Ca^{2+}]_i$ in the absence of $InsP_3$, by patch clamping isolated *Xenopus* oocyte nuclei. For both endogenous *Xenopus* type 1 and recombinant rat type 3 $InsP_3R$ channels, spontaneous $InsP_3$-independent channel activities with low open probability P_o (~0.03) were observed in $[Ca^{2+}]_i < 5$ nM with the same frequency as in the presence of $InsP_3$, whereas no activities were observed in 25 nM Ca^{2+}. These results establish the half-maximal inhibitory $[Ca^{2+}]_i$ of the channel to be 1.2–4.0 nM in the absence of $InsP_3$, and demonstrate that the channel can be active when all of its ligand-binding sites (including $InsP_3$) are unoccupied. In the simplest allosteric model that fits all observations in nuclear patch-clamp studies of $[Ca^{2+}]_i$ and $InsP_3$ regulation of steady-state channel gating behavior of types 1 and 3 $InsP_3R$ isoforms, including spontaneous $InsP_3$-independent channel activities, the tetrameric channel can adopt six different conformations, the equilibria among which are controlled by two inhibitory and one activating Ca^{2+}-binding and one $InsP_3$-binding sites in a manner outlined in the Monod-Wyman-Changeux model. $InsP_3$ binding activates gating by affecting the Ca^{2+} affinities of the high-affinity inhibitory sites in different conformations, transforming it into an activating site. Ca^{2+} inhibition of $InsP_3$-liganded channels is mediated by an $InsP_3$-independent low-affinity inhibitory site. The model also suggests that besides the ligand-regulated gating mechanism, the channel has a ligand-independent gating mechanism responsible for maximum channel P_o being less than unity. The validity of this model was established by its successful quantitative prediction of channel behavior after it had been exposed to ultra-low bath $[Ca^{2+}]$.

KEY WORDS: single-channel electrophysiology • patch clamp • calcium • *Xenopus* oocyte • nucleus

INTRODUCTION

In many cell types, the second messenger inositol 1,4,5-trisphosphate ($InsP_3$) is generated in the cytoplasm in response to the binding of extracellular ligands to plasma membrane receptors. $InsP_3$ binds to its receptor, the $InsP_3R$, in the ER and activates it as a Ca^{2+} channel to liberate stored Ca^{2+} from the ER lumen into the cytoplasm. This rapid release of Ca^{2+} modulates the cytoplasmic free Ca^{2+} concentration ($[Ca^{2+}]_i$), which serves as a ubiquitous cellular signal that can be manifested temporally as repetitive spikes or oscillations, and spatially as propagating waves or highly localized events (Meyer and Stryer, 1991; Berridge, 1993; Toescu, 1995). The temporal and spatial complexity of this signaling system involves sophisticated regulation of the activity of the $InsP_3R$ by various mechanisms, including cooperative activation by $InsP_3$ (Meyer et al., 1988; Mak et al., 1998) and biphasic feedback from the permeant Ca^{2+} ion (Iino, 1990; Bezprozvanny et al., 1991; Mak et al., 1998).

A family of three $InsP_3$ receptor isoforms has been identified—types 1, 2, and 3, with different primary sequences derived from different genes (Patel et al., 1999). Recent studies have demonstrated that channel P_o of both the types 1 and 3 $InsP_3R$ isoforms is modulated with biphasic dependencies on cytoplasmic free Ca^{2+} concentration ($[Ca^{2+}]_i$), suggesting that the channels have two distinct types of functional Ca^{2+}-binding sites: activating and inhibitory (Mak et al., 1998, 2001b). $InsP_3$ activates the $InsP_3R$ by tuning the sensitivity of the channel to Ca^{2+} inhibition, with increases in the cytoplasmic concentration of $InsP_3$ ($[InsP_3]$) causing a decrease in the apparent Ca^{2+} affinity of the inhibitory binding sites of the channel. Nevertheless, the fully $InsP_3$-liganded channel can still be inhibited

The online version of this paper contains supplemental material.

Address correspondence to J. Kevin Foskett, Department of Physiology, B39 Anatomy-Chemistry Bldg/6085, University of Pennsylvania, Philadelphia, PA 19104-6085. Fax: (215) 573-6808; email: foskett@mail.med.upenn.edu

Abbreviations used in this paper: $InsP_3$, inositol 1,4,5-trisphosphate; $InsP_3R$, $InsP_3$ receptor; *X*-$InsP_3R$-1, *Xenopus* type 1 $InsP_3R$; r-$InsP_3R$-3, rat type 3 $InsP_3R$; P_o, open probability.

by Ca^{2+}, albeit at sufficiently high concentrations (Mak et al., 1998, 2001b). Importantly, $InsP_3$ has little apparent effect on activation parameters (half-maximal activation $[Ca^{2+}]_i$, K_{act}; and activation Hill coefficient, H_{act}) of the biphasic Hill equation that describes the Ca^{2+} response of the channel, nor does it affect the robust maximum open probability exhibited by either $InsP_3R$ isoform under optimal activating conditions.

Whereas previous studies provided estimates of the affinity of the inhibitory Ca^{2+}-binding sites in subsaturating and saturating concentrations of $InsP_3$ (Mak et al., 1998, 2001b), the apparent affinity of the inhibitory Ca^{2+}-binding sites of an $InsP_3R$ channel in the absence of $InsP_3$ has not been determined. The effects of $InsP_3$ have been modeled empirically assuming infinitely high affinity of the Ca^{2+} inhibition sites in a channel not bound to $InsP_3$ (Mak et al., 1998, 2001b), but it is more reasonable to expect that the inhibitory Ca^{2+}-binding sites adopt a finite maximal Ca^{2+} affinity in the absence of $InsP_3$.

Here, we examined activities of the types 1 and 3 $InsP_3R$ channels in the absence of $InsP_3$ to characterize the apparent affinity of the inhibitory Ca^{2+}-binding site of the $InsP_3R$ not bound to $InsP_3$. We reasoned that since $InsP_3$ activates the channel by preventing Ca^{2+} from inhibiting it, it might be possible to activate the channel in the absence of $InsP_3$ by removing Ca^{2+} from the inhibitory site by simply reducing $[Ca^{2+}]_i$ to very low levels. We demonstrate that the $InsP_3R$ channel opens spontaneously in the absence of $InsP_3$ when the channel is exposed to $[Ca^{2+}]_i < 5$ nM, but not when $[Ca^{2+}]_i$ is elevated to 25 nM. These observations establish the apparent affinity of the Ca^{2+} inhibition sites of an $InsP_3R$ channel not bound to $InsP_3$, and they support an allosteric model of $InsP_3R$ activation by Ca^{2+}.

Many models have been developed to account for $InsP_3R$-mediated $[Ca^{2+}]_i$ signals, but all previously proposed models of $InsP_3R$ single-channel gating (De Young and Keizer, 1992; Swillens et al., 1994; Kaftan et al., 1997; Marchant and Taylor, 1997; Swillens et al., 1998; Adkins and Taylor, 1999; Moraru et al., 1999) assumed that only the $InsP_3$-bound state(s) of the receptor is active. Thus, they fail to account for the spontaneous, $InsP_3$-independent activities of the $InsP_3R$ observed in our study. To provide insights into the mechanisms underlying ligand regulation of $InsP_3R$ channel activity, we have developed an allosteric molecular model that can quantitatively account for not only the spontaneous, $InsP_3$-independent channel activities in low $[Ca^{2+}]_i$, but all other characteristics of $InsP_3$ and $[Ca^{2+}]_i$ regulation of both types 1 and 3 $InsP_3R$ isoforms observed in nuclear patch clamp experiments (Mak et al., 1998, 2001b, 2003).

MATERIALS AND METHODS

Selection and Microinjection of Xenopus Oocytes

Maintenance of *Xenopus laevis* and surgical extraction of ovaries were performed as previously described (Jiang et al., 1998). The level of endogenous $InsP_3R$ channel activity was determined for each new batch of oocytes by patch clamping at least 3 isolated nuclei, obtaining 4–6 patches from each (Mak et al., 2000, 2001b). Rat type 3 $InsP_3R$ (r-$InsP_3R$-3) channels were expressed by cRNA injection into oocytes ascertained to have extremely low level of endogenous $InsP_3R$ activities. In these studies, one endogenous *Xenopus* oocyte type 1 $InsP_3R$ (*X*-$InsP_3R$-1) channel was observed in 100 patches from 5 batches of oocytes used for r-$InsP_3R$-3 cRNA injection. In contrast, 544 channels were detected in 330 membrane patches, with 108 patches containing multiple $InsP_3R$ channels, from nuclei of r-$InsP_3R$-3-expressing oocytes 4–5 d after cRNA injection. Assuming that the types 1 and 3 $InsP_3R$ associate randomly to form tetrameric channels, 97.6% of $InsP_3R$ channels detected in these experiments were contributed by type 3 homotetramers (Mak et al., 2000).

The endogenous *X*-$InsP_3R$-1 was studied using batches of oocytes with high level of endogenous $InsP_3R$ activities, up to four days after ovary extraction (Mak and Foskett, 1994, 1997, 1998).

Patch Clamp Data Acquisition and Analysis

Patch clamp electrophysiology of isolated nuclei was performed as described (Mak and Foskett, 1994, 1997, 1998; Mak et al., 2000) in "on-nucleus" configuration at room temperature with the pipette electrode at +20 mV (unless stated otherwise) relative to the reference bath electrode. Transmembrane currents were amplified, filtered at 1 kHz, digitized at 5 kHz and recorded directly onto hard disk.

Channel opening and closing events were identified with a 50% threshold, and channel open probabilities and mean open and closed durations, were evaluated using MacTac software (Bruxton). The number of channels in the membrane patch was assumed to be the maximum number of open channel current levels observed throughout the current record (Mak et al., 2001b). When low channel open probability ($P_o < 0.1$) was observed, generally only current records lasting >30 s and exhibiting only one open channel current level were used in our analyses to avoid under-estimating the total number of active $InsP_3R$ channels present in the membrane patch, which would lead to over-estimation of channel P_o.

The data points shown for each set of experimental conditions are the means of results from at least four separate patch-clamp experiments performed under the same conditions. Error bars indicate the SEM.

Iterative fitting of the experimentally obtained channel P_o in various $[InsP_3]$ and $[Ca^{2+}]_i$ by the different molecular models were performed using Igor Pro software (WaveMetrics) with a nonlinear least-square fit (Levenberg-Marquardt) algorithm.

Solutions for Patch Clamp Experiments

All pipette solutions used in patch clamp experiments contained 140 mM KCl and 10 mM HEPES, except the low KCl solutions, which contained 14 mM KCl and 1 mM HEPES. The pipette solutions were pH adjusted to 7.3 with KOH.

By using K1 as the current carrier and appropriate quantities of the high-affinity Ca^{2+} chelator, BAPTA (1,2-bis(*O*-aminophenoxy) ethane-*N,N,N′,N′*-tetraacetic acid; Molecular Probes) (500–1,000 μM), Ca^{2+} concentrations in our experimental solutions were tightly controlled (Mak et al., 2003). For solutions

with free $[Ca^{2+}] > 10$ nM, free $[Ca^{2+}]$ was directly measured using Ca^{2+}-selective minielectrodes (Baudet et al., 1994). For experimental solutions with $[Ca^{2+}] < 10$ nM, the total $[Ca^{2+}]$ was determined by induction-coupled plasma mass spectrometry (Mayo Medical Laboratory) to be 6–10 μM. In the presence of 1 mM BAPTA in 140 mM KCl, 10 mM HEPES and 0.5 mM ATP at pH 7.3, the $[Ca^{2+}]_i$ was calculated to be 0.9–1.5 nM using the Maxchelator software (C. Patton, Stanford University, Stanford, CA). Direct measurement by Ca^{2+}-selective electrode confirmed the free $[Ca^{2+}]$ to be <5 nM, but the accuracy of this measurement was limited by the nonlinearity of the calibration curve of the electrode in such low free $[Ca^{2+}]$.

Pipette solutions contained various concentrations of Na_2ATP, either 0 or 10 μM of $InsP_3$ (Molecular Probes) and either 0 or 100 μg/ml heparin (Sigma-Aldrich) as stated.

The bath solutions used in all experiment had 140 mM KCl, 10 mM HEPES, 300 μM $CaCl_2$, 500 μM BAPTA (measured $[Ca^{2+}] \approx$ 400–500 nM), and pH 7.3.

Online Supplemental Material

The online supplemental material provides details, descriptions, and derivations of the allosteric models (both Monod-Wyman-Changeux [MWC] based and non-MWC–based models) that were considered to describe the ligand regulation of the $InsP_3R$ channel gating. The mathematical derivations from first principles of the equations used to calculate the theoretical $InsP_3R$ channel P_o according to each of those models are presented, and comparisons between the calculated channel P_o and experimental data under selected conditions are discussed. Online supplemental material is available at http://www.jgp.org/cgi/content/full/jgp.200308809/DC1.

RESULTS

Regulation of Types 1 and 3 $InsP_3R$ Channel P_o by Cytoplasmic Ca^{2+}, $InsP_3$ and ATP

Single *X*-$InsP_3R$-1 and r-$InsP_3R$-3 channels observed in the same nuclear membrane system exhibit biphasic regulation by $[Ca^{2+}]_i$, with open probabilities (P_o) well described by the empirical biphasic Hill equation (Mak et al., 1998, 2001b):

$$P_o = P_{max}\left\{1 + (K_{act}/[Ca^{2+}]_i)^{H_{act}}\right\}^{-1}\left\{1 + ([Ca^{2+}]_i/K_{inh})^{H_{inh}}\right\}^{-1} \quad (1)$$

where P_{max} is the maximum channel open probability that can be achieved by the $InsP_3R$ channel under optimal $[Ca^{2+}]_i$ and saturating $[InsP_3]$, K_{act} is the half-maximal activating $[Ca^{2+}]_i$, H_{act} is the activation Hill coefficient, K_{inh} is the half-maximal inhibitory $[Ca^{2+}]_i$, and H_{inh} is the inhibition Hill coefficient.

In nuclear patch clamp experiments, both $InsP_3R$ isoforms achieve a robust P_{max} of 0.8 under optimal conditions. *X*-$InsP_3R$-1 and r-$InsP_3R$-3 channels both exhibit similar inhibition by Ca^{2+}: K_{inh} in the presence of saturating $[InsP_3]$ is ~40–50 μM, and H_{inh} is ~3–4, indicating that the Ca^{2+} inhibition process is highly cooperative. $InsP_3$ activates both channel isoforms by increasing K_{inh}, i.e., decreasing the sensitivity of the channel to Ca^{2+} inhibition, with no effect on the other Hill equation parameters (P_{max}, H_{inh}, K_{act} or H_{act}) (Mak et al., 1998, 2001b). In the presence of 0.5 mM free ATP, the $InsP_3$-concentration dependence of K_{inh} of each $InsP_3R$ isoform can be described empirically by a simple Hill equation (Mak et al., 1998, 2001b):

$$K_{inh} = K_{inh}^{\infty}\{1 + (K_{IP3}/[InsP_3])^{H_{IP3}}\}^{-1} \quad (2)$$

with similar parameters: the half-maximal activating $[InsP_3]$ (K_{IP3}) ~50 nM, the Hill coefficient (H_{IP3}) ~4, and the maximum half-maximal inhibitory $[Ca^{2+}]_i$ at saturating $[InsP_3]$ (K_{inh}^{∞}) ~45 μM.

Since the affinity of the inhibitory Ca^{2+}-binding site must be finite even in the absence of $InsP_3$, we hypothesized that the $InsP_3$ requirement for channel activities could be waived if Ca^{2+} could be dissociated from the inhibitory Ca^{2+}-binding site by an $InsP_3$-independent method. Although one straight-forward method to accomplish this would be by lowering $[Ca^{2+}]_i$, channel opening requires Ca^{2+} binding to Ca^{2+} activation sites. We speculated that $InsP_3$-independent channel activities should occur in low $[Ca^{2+}]_i$ conditions in which Ca^{2+} would dissociate only from the inhibitory sites but not from the activating sites. Thus, we attempted to determine if simply dissociating Ca^{2+} from the inhibitory sites would be sufficient to activate channel opening, by using experimental conditions in which the affinity of the activating Ca^{2+}-binding site was as high as possible. It was previously demonstrated that cytoplasmic free ATP acid (ATP^{3-} and ATP^{4-}) markedly enhances the Ca^{2+} affinity of the activation sites in both isoforms (Mak et al., 1998, 2001b). In saturating (10 μM) $InsP_3$, the r-$InsP_3R$-3 in 0.5 mM ATP and the *X*-$InsP_3R$-1 in 9.5 mM ATP both exhibit a moderate P_o of 0.2–0.4 in the presence of very low (25 nM) $[Ca^{2+}]_i$ (Mak et al., 1999, 2001a). Thus, the requirement for Ca^{2+} binding to the Ca^{2+} activation site is satisfied at this Ca^{2+} concentration under these conditions. We reasoned that if the minimum value of K_{inh} of the channel is not too low (for example, >20 nM), then $InsP_3R$ channel activity should be observable at 25 nM Ca^{2+} in appropriate [ATP] even in the absence of $InsP_3$.

Lack of Channel Activity at 25 nM Ca^{2+} for $InsP_3R$ Not Bound to $InsP_3$

A series of experiments was performed with membrane patches obtained from the same areas (±2 μm) of isolated nuclei from uninjected oocytes, where clustering of endogenous *X*-$InsP_3R$-1 channels gave an exceptionally high probability of observing channel activity in membrane patches (Mak and Foskett, 1997). The pipette solutions alternately contained either 25 nM Ca^{2+}, no $InsP_3$, and 9.5 mM free ATP; or 1,150 nM

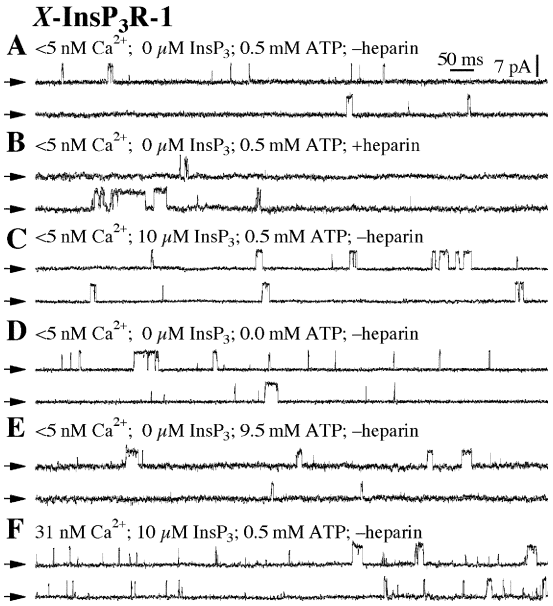

FIGURE 1. Typical single-channel current traces of *X*-$InsP_3R$-1 channels in various $[Ca^{2+}]_i$, [ATP] and [$InsP_3$], as labeled. Arrows indicate closed channel current levels. 100 μg/ml heparin was used in +heparin experiments.

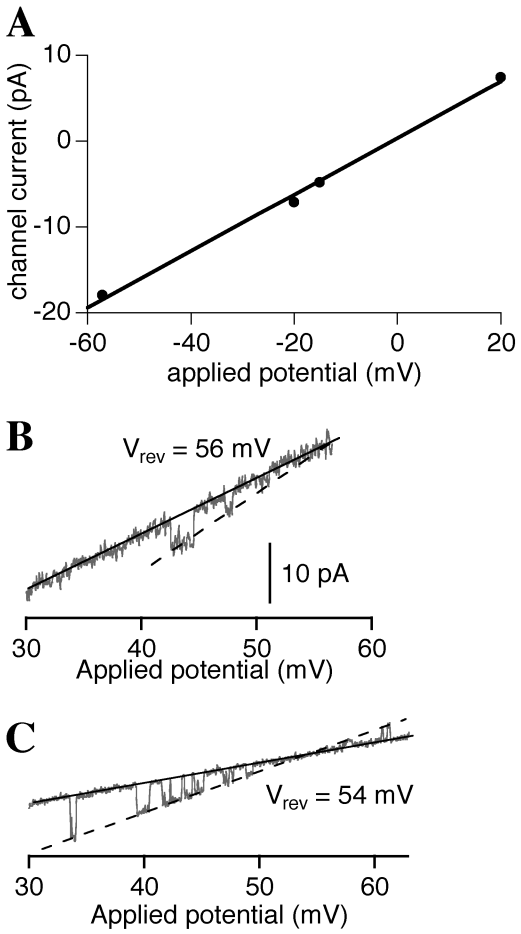

FIGURE 2. (A) Channel current versus applied transmembrane potential curve for $InsP_3R$ channels ($n = 4$) observed in symmetric 140 mM KCl in the presence of $[Ca^{2+}]_i < 5$ nM, 0.5 mM ATP and no $InsP_3$. (B and C) Current traces with $InsP_3R$ channel observed under an applied potential ramp in 140 mM KCl bath and 14 mM KCl pipette solutions. For B, pipette solution contained $[Ca^{2+}]_i <$ 5 nM, 0.5 mM ATP and no $InsP_3$, whereas for C, pipette solution contained 1 μM $[Ca^{2+}]_i$, 0.5 mM ATP and 10 μM $InsP_3$. The slope conductances of the channels were evaluated as the difference between the slopes of the open (dashed line) and closed (solid line) channel current levels. The positive reversal potentials (as tabulated in the graphs) indicate that the $InsP_3R$ channels observed are cation selective.

Ca^{2+}, 10 μM $InsP_3$, and 0.5 mM ATP. The latter solution is one that maximizes the P_o of the channel (Mak et al., 1998), and was therefore used to ensure that lack of channel activities in the former solution was not due to absence of $InsP_3R$ in the patched membranes. Whereas *X*-$InsP_3R$-1 channel activities were detected in all eight patches with pipette solutions containing 10 μM $InsP_3$, no channel activity was observed in any of the 26 patches with pipette solutions lacking $InsP_3$. Thus, the type 1 channel cannot open in the absence of $InsP_3$ in 25 nM Ca^{2+}. In a parallel series of experiments using nuclei from r-$InsP_3R$-3–expressing oocytes, in which the expressed recombinant channels exhibit similar clustering (Mak et al., 2000), no r-$InsP_3R$-3 channel activity was detected in any of the eight patches with pipette solutions lacking $InsP_3$, even though r-$InsP_3R$-3 channel activities were observed in all seven patches with pipette solutions that contained 10 μM $InsP_3$. These results therefore suggested that the apparent K_{inh} in the absence of $InsP_3$ (K^0_{inh}) for both the *X*-$InsP_3R$-1 and r-$InsP_3R$-3 channel isoforms is lower than 25 nM.

$InsP_3$-independent Activity of X-$InsP_3R$-1 at Ultra-low $[Ca^{2+}]_i$

When $[Ca^{2+}]_i$ was further decreased to <5 nM (calculated to be 0.9–1.5 nM, see MATERIALS AND METHODS), with no $InsP_3$ and 0.5 mM ATP in the pipette solution, channel activities with low open probability of ~0.03, and with conduction and gating properties very similar to those of the $InsP_3R$ were observed in nuclei from uninjected oocytes (Fig. 1 A). Even though these channel activities were observed in the absence of $InsP_3$, several characteristics identified them as being contributed by the endogenous *X*-$InsP_3R$-1. First, the most frequently observed (>90%) channel conductance was 330 ± 15 pS (Fig. 2 A), indistinguishable from that of the $InsP_3$-activated *X*-$InsP_3R$-1 channels observed in the same system (Mak and Foskett, 1998). Importantly, no channel activities with conductances between 100 and 450 pS have been observed previously in the absence of $InsP_3$ in thousands of nuclear patch clamp recordings on isolated oocyte nuclei (Mak and Foskett, 1998; Mak et al.,

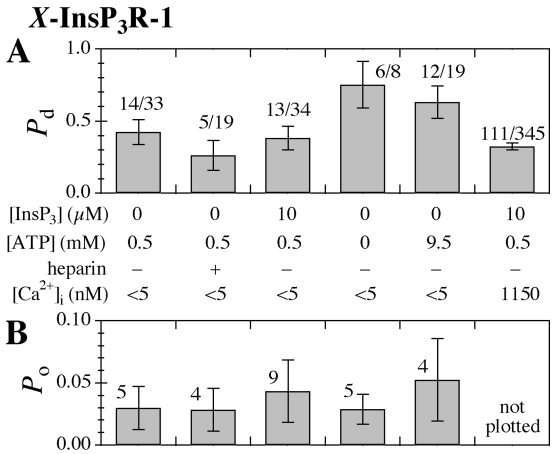

FIGURE 3. (A) P_d and (B) P_o histograms of the *X*-InsP$_3$R-1 channel in various experimental conditions. In the P_d graph, numbers above each bar represent the fraction of nuclear membrane patches obtained that exhibited *X*-InsP$_3$R-1 channel activities. In the P_o graph, the number above each bar is the number of single-channel current records used to evaluate P_o. Given the variance of the channel P_o in experiments performed under the same experimental conditions, the channel P_o observed under the various set of experimental conditions are not statistically different ($P > 0.05$ from *t* test) from P_o observed under control conditions (0 InsP$_3$, 0.5 mM ATP, $[Ca^{2+}]_i < 5$ nM).

1998). Second, although the P_o of the *X*-InsP$_3$R-1 channel has a strong $[Ca^{2+}]_i$-dependence, the mean channel open duration $<\tau_o>$ lies within a narrow range (3–12 ms) in all the various experimental conditions previously investigated (Mak et al., 1998, 1999). $<\tau_o>$ of the channel activities observed in < 5 nM $[Ca^{2+}]_i$ was 3.4 ± 0.4 ms (Fig. 1 A), which is within the normal narrow range of $<\tau_o>$ exhibited by *X*-InsPR$_3$-1 channels (Fig. 1 F). Third, the probability of observing this channel activity in a membrane patch (P_d) in these experimental conditions was similar to that in the same nucleus with pipettes containing an optimal activating solution (1,150 nM Ca^{2+}, 10 μM InsP$_3$, and 0.5 mM ATP; Fig. 3 A). Fourth, both the slope conductance (365 ± 20 pS) and reversal potential (56 ± 2 mV) of the channel observed in <5 nM $[Ca^{2+}]_i$ and 0 InsP$_3$ (Fig. 2 B) in the presence of asymmetric KCl conditions (14 mM KCl in the pipette and 140 mM KCl in bath) were very similar to those values (312 ± 20 pS and 54 ± 2 mV, respectively) observed for InsP$_3$R channel under similar ionic conditions in the presence of 1 μM $[Ca^{2+}]_i$ and 10 μM [InsP$_3$] (Fig. 2 C). This indicates that the channel responsible for the activities observed in the absence of InsP$_3$ has the same channel conductance and cation selectivity as the InsP$_3$R channel under the same ionic conditions. Together, these observations render it highly unlikely that the channel activities observed in <5 nM $[Ca^{2+}]_i$ were due to channels other than the *X*-InsP$_3$R-1.

The observations of InsP$_3$-independent channel activities support our working hypothesis that ligand-independent channel activity can be achieved under conditions that dissociate Ca^{2+} from the inhibitory Ca^{2+}-binding site. A further prediction of this hypothesis is that not only is InsP$_3$ not necessary for channel activities under ultra-low $[Ca^{2+}]_i$ conditions, but that channel activities will in fact be insensitive to InsP$_3$. To investigate the dependence on InsP$_3$ of InsP$_3$R-1 channel activity in <5 nM $[Ca^{2+}]_i$, we used pipette solutions containing either 10 μM InsP$_3$, or no InsP$_3$. To rule out effects of possible contaminating InsP$_3$ present in our system, 100 μg/ml heparin, a competitive inhibitor of InsP$_3$ binding to the InsP$_3$R (Worley et al., 1987; Cullen et al., 1988), was used in the pipette solution with no InsP$_3$. Similar channel activities were observed (Fig. 1, B and C) with comparable P_d as in the absence of InsP$_3$ (Fig. 3 A). In addition, there was no systematic or statistically significant difference in the single-channel P_o (~0.03) in the presence or absence of InsP$_3$ and heparin (Fig. 3 B). Thus, the *X*-InsP$_3$R-1 has a low but nonzero P_o at <5 nM $[Ca^{2+}]_i$ regardless of whether the InsP$_3$-binding site is occupied or not. This result suggests that the inhibitory Ca^{2+}-binding sites of the channel was mostly unoccupied at $[Ca^{2+}]_i < 5$ nM regardless of the [InsP$_3$].

Of note, because $K_{act} = 190$ nM in 0.5 mM ATP (Mak et al., 1998), the activating Ca^{2+}-binding site of the *X*-InsP$_3$R-1 channel was also effectively unoccupied when $[Ca^{2+}]_i < 5$ nM. This result suggests that the spontaneous channel activity can occur when both the activating as well as the inhibitory Ca^{2+} sites are un-liganded. Because ATP stimulates channel activities by enhancing the functional affinity of the activating Ca^{2+}-binding sites (Mak et al., 1999), the fact that the activating Ca^{2+}-binding sites remain effectively unoccupied in <5 nM Ca^{2+} predicts that the InsP$_3$-independent channel activities should be unaffected by ATP. In agreement, channel activities with similar conductances were observed regardless of [ATP] (0–9.5 mM; Fig. 1, A, D, and E). Neither P_d nor P_o of the *X*-InsP$_3$R-1 channel in the absence of InsP$_3$ were significantly affected by [ATP] (Fig. 3, $P > 0.05$). Together, these results demonstrate that the *X*-InsP$_3$R-1 channel has an intrinsic, low P_o even when its InsP$_3$-binding sites and activating Ca^{2+}-binding sites are not occupied, as long as its inhibitory Ca^{2+}-binding sites are unoccupied.

InsP$_3$-independent Activity of r-InsP$_3$R-3 at Ultra-low $[Ca^{2+}]_i$

Similar results were obtained for the recombinant r-InsP$_3$R-3 channels. In <5 nM $[Ca^{2+}]_i$, channel activities with conductances very similar to those of the *X*-InsP$_3$R-1 were also observed in nuclei from r-InsP$_3$R-3 cRNA-injected oocytes, independent of [InsP$_3$] (0 or 10 μM), [ATP] (0 or 0.5 mM), or the presence of heparin (100

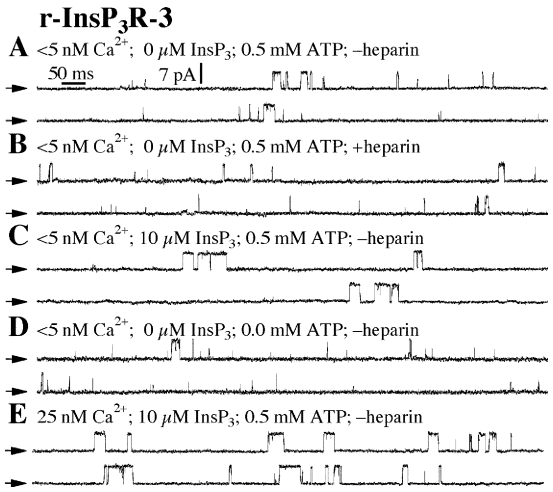

FIGURE 4. Typical single-channel current traces of r-InsP$_3$R-3 channels in various $[Ca^{2+}]_i$, [ATP] and [InsP$_3$], as labeled. Arrows indicate closed channel current levels. 100 μg/ml heparin was used in +heparin experiments.

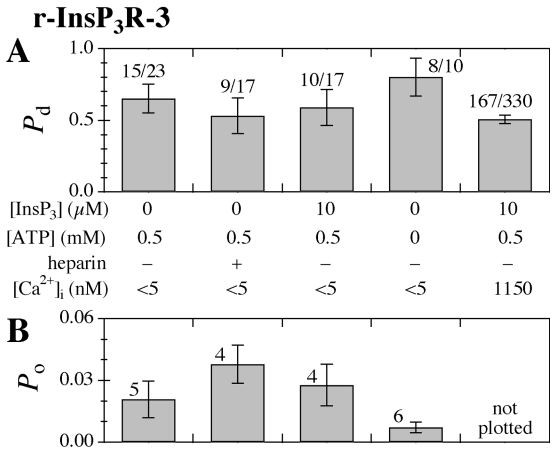

FIGURE 5. (A) P_d and (B) P_o histograms of the r-InsP$_3$R-3 channel in various experimental conditions. Numbers tabulated in the graphs have the same meanings as in Fig. 3. Given the variance of the channel P_o in experiments performed under the same experimental conditions, the channel P_o observed under the various set of experimental conditions are not statistically different ($P > 0.05$ from t test) from P_o observed under control conditions (0 InsP$_3$, 0.5 mM ATP, $[Ca^{2+}]_i < 5$ nM).

μg/ml) (Fig. 4, A–D). Also similar to the *X*-InsP$_3$R-1, the P_o of the r-InsP$_3$R-3 channel at <5 nM $[Ca^{2+}]_i$ exhibited no systematic or statistically significant dependence ($P > 0.05$) on [InsP$_3$] or [ATP] (Fig. 5 B). $<\tau_o>$ of the observed type 3 channels were 3.5–9 ms, very similar to the $<\tau_o>$ of 3–20 ms exhibited by the channel in the presence of InsP$_3$ (comparing Fig. 4, A–D, with Fig. 4 E). P_d of the channel activities at $[Ca^{2+}]_i < 5$ nM under various [InsP$_3$] and [ATP] were similar to that for experiments using the same cRNA-injected oocyte nuclei with a pipette solution containing 1,150 nM Ca^{2+}, 10 μM InsP$_3$, and 0.5 mM ATP (Fig. 5 A). These results indicate that, similar to the *X*-InsP$_3$R-1, the inhibitory Ca^{2+}-binding sites of r-InsP$_3$R-3 are mostly unoccupied in $[Ca^{2+}]_i < 5$ nM, and the r-InsP$_3$R-3 channel has a low but nonzero P_o even when its InsP$_3$-binding sites and activating Ca^{2+}-binding sites are not occupied, as long as its inhibitory Ca^{2+}-binding sites are also unoccupied.

DISCUSSION

Finite Affinity of the Inhibitory Ca^{2+}-binding Sites in InsP$_3$R Channels

This study has revealed that InsP$_3$R channels can be active spontaneously in the absence of InsP$_3$ when $[Ca^{2+}]_i$ is lowered to <5 nM, but not when it is lowered only to 25 nM. These observations suggest that the inhibitory Ca^{2+} sites were mostly unoccupied at <5 nM $[Ca^{2+}]_i$, whereas they were occupied when $[Ca^{2+}]_i$ was 25 nM. The lack of occupancy of the inhibitory Ca^{2+} sites at <5 nM $[Ca^{2+}]_i$ obviated the requirement for InsP$_3$ binding, enabling the channel to open in the absence of the physiological ligand. These results support a model in which InsP$_3$ binding activates InsP$_3$R channel by reducing the apparent affinity of inhibitory Ca^{2+}-binding sites (Mak et al., 1998), and they have implications for our understanding of the molecular mechanisms that regulate channel activity.

To provide a better empirical description of the tuning by [InsP$_3$] of the channel sensitivity to Ca^{2+} inhibition that incorporates our present observations, the simple Hill equation describing the effects of InsP$_3$ (Eq. 2) has to be modified to:

$$K_{inh} = K^0_{inh} + (K^\infty_{inh} - K^0_{inh})\{1 + (K_{IP3}/[InsP_3])^{H_{IP3}}\}^{-1} \quad (3)$$

where K^0_{inh} is the nonzero minimum K_{inh} in the absence of InsP$_3$. The empirical biphasic Hill equation describing the Ca^{2+} dependence of the P_o of the InsP$_3$R (Eq. 1) also has to be modified to:

$$P_o = \left\{P^0_{max} + (P^\infty_{max} - P^0_{max})\right. \quad (4)$$

$$\left.[1 + (K_{act}/[Ca^{2+}]_i)^{H_{act}}]^{-1}\right\}[1 + ([Ca^{2+}]_i/K_{inh})^{H_{inh}}]^{-1},$$

with P^0_{max} and P^∞_{max} being the maximum P_o when the activating Ca^{2+} sites are unoccupied or fully occupied, respectively. Because the values of P^∞_{max}, H_{act}, H_{inh}, and K_{act} in the presence of various [ATP] have already been obtained in our previous studies for *X*-InsP$_3$R-1 (Mak et al., 1998, 1999) and r-InsP$_3$R-3 (Mak et al., 2001a,b), the channel P_o for various $[Ca^{2+}]_i$, [InsP$_3$] and [ATP] can be evaluated using Eqs. 3 and 4. Therefore, even

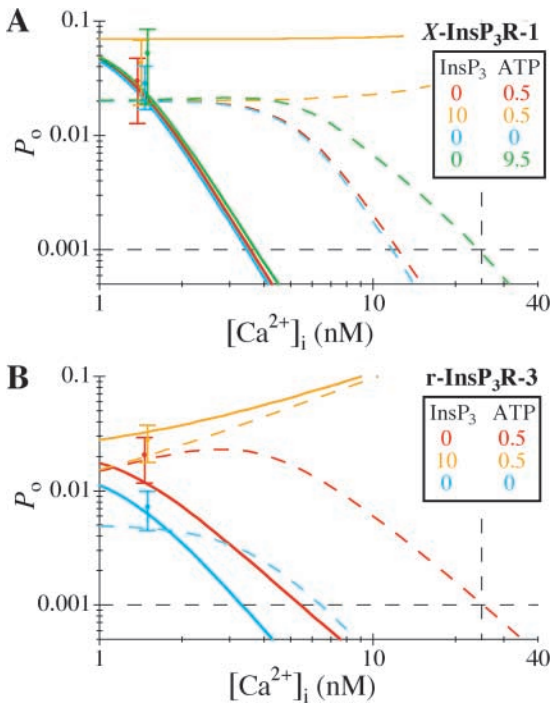

FIGURE 6. Estimating K^0_{inh} and P^0_{max} from channel activities at low $[Ca^{2+}]_i$ for (A) *X*-InsP$_3$R-1 and (B) r-InsP$_3$R-3. Different colors correspond to different InsP$_3$ and ATP concentrations as tabulated in the graphs. InsP$_3$R channel P_o observed in calculated $[Ca^{2+}]_i$ of 0.9–1.5 nM are plotted as data points at $[Ca^{2+}]_i$ = 1.5 nM (c.f. Figs. 3 B and 5 B). InsP$_3$R channel P_o at various $[Ca^{2+}]_i$ can be calculated with Eq. 4 using the values of P^∞_{max}, K_{act}, H_{act}, and H_{inh} obtained in our previous studies for *X*-InsP$_3$R-1 (Mak et al., 1998, 1999) and r-InsP$_3$R-3 (Mak et al., 2001a,b). The values of parameters K^0_{inh} and P^0_{max} in Eq. 4, which were not determined in previous experiments, must be constrained so that: (a) the calculated channel P_o at various InsP$_3$ and ATP concentrations agree with experimental observations (i.e., lie within the error limits of the data points at 1.5 nM $[Ca^{2+}]_i$), and (b) the calculated channel P_o in the absence of InsP$_3$ is <0.001 at 25 nM $[Ca^{2+}]_i$, so that no channel activity was detected at 25 nM $[Ca^{2+}]_i$. The continuous and dashed curves represent channel P_o calculated using two extreme sets of values for K^0_{inh} and P^0_{max} that satisfy those requirements. For *X*-InsP$_3$R-1, the continuous curves are calculated with P^0_{max} = 0.07 and K^0_{inh} = 1.2 nM; and the dashed curves are calculated with P^0_{max} = 0.02 and K^0_{inh} = 5.5 nM. For r-InsP$_3$R-3, the continuous curves are calculated with P^0_{max} = 0.018 and K^0_{inh} = 1.2 nM; and the dashed curves are calculated with P^0_{max} = 0.005 and K^0_{inh} = 3.8 nM. The observed channel P_o data points in both graphs and the continuous curves in A are slightly offset along the $[Ca^{2+}]_i$ axis for easier visualization.

though the values of K^0_{inh} and P^0_{max} are not precisely defined by our observations of spontaneous ligand-independent InsP$_3$R channel activities, they can nevertheless be estimated using the constraints derived from our observations. First, even in the presence of optimal ATP concentrations, there were no detectable InsP$_3$R channel activities in 25 nM $[Ca^{2+}]_i$ in the absence of InsP$_3$. Because of the technical limitations of the experimental system, channel activity with $P_o < 0.001$ is not detectable in our experiments. Thus, the P_o must be lower than 0.001 (marked by the horizontal dashed lines in Fig. 6) in 25 nM $[Ca^{2+}]_i$ (marked by the vertical dashed lines in Fig. 6) in the absence of InsP$_3$. Second, both InsP$_3$R isoforms exhibited channel activities in 0.9–1.5 nM $[Ca^{2+}]_i$ in various InsP$_3$ and ATP concentrations with P_o as shown in Figs. 3 B and 5 B. The observed *X*-InsP$_3$R-1 channel P_o are consistent with those calculated from Eqs. 3 and 4 using P^0_{max} = 0.02–0.07, and K^0_{inh} = 1.2–5.5 nM (Fig. 6 A). Similarly, experimental r-InsP$_3$R-3 channel P_o agree with those calculated from Eqs. 3 and 4 using P^0_{max} = 0.005–0.018, and K^0_{inh} = 1.2–3.8 nM (Fig. 6 B).

If the InsP$_3$R channel can be active in the absence of InsP$_3$ binding, how can high fidelity Ca^{2+} release responses be achieved during cellular signaling? Although InsP$_3$R channels can exhibit InsP$_3$-independent activities, such spontaneous activities only occur in the presence of ultra-low $[Ca^{2+}]_i$ (<25 nM), levels unlikely to be achieved under physiological conditions. Therefore, although the detection of the InsP$_3$-independent spontaneous channel activities provides insights into the molecular bases for the complex regulation of the channel by Ca^{2+} and InsP$_3$ (discussed below), such spontaneous activities by themselves probably have limited physiological implications in intracellular Ca^{2+} signaling. However, the regulation of the channel can now be viewed as a complex strategy designed to prevent spontaneous Ca^{2+} release while satisfying competing requirements of the channel. First, the channel requires Ca^{2+}-induced Ca^{2+} release (CICR) properties to enable it to amplify and propagate $[Ca^{2+}]_i$ signals. Conversely, the activity of the channel must be highly controlled to enable it to provide signals with high temporal and spatial specificity and fidelity. By using Ca^{2+} as a high-affinity inhibitor of channel activity, the channel is provided with a mechanism to prevent spontaneous channel activity from triggering inappropriate CICR. By using InsP$_3$ as a negative regulator of Ca^{2+} inhibition, the channel is provided with a mechanism to ensure graded Ca^{2+} release activity with high temporal specificity in response to cellular signals.

Toward an Allosteric Model for the Regulation of InsP$_3$R Channel Activities by $[Ca^{2+}]_i$ and InsP$_3$

Although Eqs. 3 and 4 can describe the regulation of InsP$_3$R channel P_o by its ligands Ca^{2+} and InsP$_3$, enabling the channel P_o at any $[Ca^{2+}]_i$ and [InsP$_3$] to be evaluated in terms of a set of parameters (P^0_{max}, P^∞_{max}, K_{act}, H_{act}, H_{inh}, K^0_{inh}, K^∞_{inh}, K_{IP3}, and H_{IP3}) that are deduced from experimental data, the equations are empirical and they do not provide insights into the specific molecular mechanisms underlying ligand regulation of InsP$_3$R activity. Therefore, it is desirable to develop a molecular model for ligand regulation of

$InsP_3R$ activity that can, in terms of simple molecular mechanisms, account for all the features of the regulation of $InsP_3R$ channels (both types 1 and 3 isoforms) by $[Ca^{2+}]_i$ and $[InsP_3]$ observed in extensive nuclear patch-clamp studies (Mak et al., 1998, 2001b, 2003; Boehning et al., 2001; and this study), as well as satisfy constraints imposed by the known structure of the $InsP_3R$ molecule and channel.

The observations, for both types 1 and 3 isoforms, that must be accounted for in such a molecular model are as follows:

(i) The $InsP_3R$ channel can be active when none of its ligand-binding sites are occupied ($[InsP_3] = 0$ and $[Ca^{2+}]_i$ = 1.5–2 nM << K_{act} and K_{inh}). Spontaneous activities of the $InsP_3R$ channel in the absence of all ligands observed in the present study are reminiscent of the spontaneous activities observed in the acetylcholine receptor channel (Jackson, 1984) and cyclic nucleotide–gated channels (Picones and Korenbrot, 1995). In those channels, ligand-independent gating suggested that allosteric models, in which the channel has a nonzero probability of being open even when its ligand-binding sites are unoccupied, were more appropriate than schemes that assume ligand binding to be necessary for channel opening. The ligand-independent opening of the $InsP_3R$ channels observed here cannot be accounted for by previously proposed models of $InsP_3R$ single-channel gating (De Young and Keizer, 1992; Swillens et al., 1994; Kaftan et al., 1997; Marchant and Taylor, 1997; Swillens et al., 1998; Adkins and Taylor, 1999; Moraru et al., 1999), in which only the $InsP_3$-bound state(s) of the receptor is assumed to be active. Instead, our new observations suggest that an allosteric model in which the $InsP_3R$ channel has a finite probability of being open even when its activating Ca^{2+} and $InsP_3$ binding sites are unoccupied (Monod et al., 1965) probably offers a better molecular picture for the ligand activation of the $InsP_3R$. Furthermore, the model must also account for the absence of any spontaneous $InsP_3$-independent channel activities in $[Ca^{2+}]_i$ = 25 nM.

(ii) When the channel is studied in regular bath $[Ca^{2+}]$ (400–500 nM), $InsP_3$ has no effect on Ca^{2+} activation parameters (specifically K_{act} and H_{act}) in the empirical Hill equation (Eq. 2 or 4) of the channel (both isoforms). At a low $[Ca^{2+}]_i$ (for example, 100 nM), the channel P_o remains unchanged at either sub-saturating (33 nM) or saturating (10 μM) concentrations of $InsP_3$. $InsP_3$ activates the $InsP_3R$ by reducing the sensitivity of the channel to high $[Ca^{2+}]_i$ inhibition (i.e., increasing K_{inh} in Eq. 2 or 4) (Mak et al., 1998, 2001b). This lack of effect of $InsP_3$ on K_{act} and H_{act} cannot be accounted for by any previously proposed model for the $InsP_3R$ channel (De Young and Keizer, 1992; Swillens et al., 1994; Kaftan et al., 1997; Marchant and Taylor, 1997; Swillens et al., 1998; Adkins and Taylor, 1999; Moraru et al., 1999), in which $InsP_3$ binding to the channel affects Ca^{2+} binding to the activating site, and vice versa.

(iii) When studied in the presence of regular bath $[Ca^{2+}]$ (400–500 nM), $InsP_3R$ channel P_o exhibits biphasic regulation by $[Ca^{2+}]_i$ in the presence of both saturating (10 μM) as well as subsaturating (≤100 nM) $[InsP_3]$ (Mak et al., 1998, 2001b).

(iv) Ca^{2+} inhibition of $InsP_3R$ channel activity is extremely sensitive to small changes in $[InsP_3]$ when 10 nM < $[InsP_3]$ < 100 nM. When the $[InsP_3]$ is raised from 10 to 100 nM, the K_{inh} value for $InsP_3R$-1 increases by over two orders of magnitude (Mak et al., 1998). Fitting the experimentally derived K_{inh} for types 1 and 3 isoforms by Eq. 3 indicates that the empirical Hill coefficient for the $InsP_3$ dependence of K_{inh} is ∼4.

(v) The response of $InsP_3R$ channel activity to $InsP_3$ saturates very abruptly. $InsP_3R$-1 channel activity is already maximal when $InsP_3$ = 100 nM, so that the sensitivity of the channel to Ca^{2+} inhibition exhibits no discernible change when $[InsP_3]$ is further increased by over three orders of magnitude from 100 nM to 180 μM. Despite the effect of $InsP_3$ on the apparent affinity of the inhibitory Ca^{2+} sites of the $InsP_3R$, once the $InsP_3R$ is fully activated by $InsP_3$ (i.e., $[InsP_3]$ > 100 nM), the presence of a higher $[InsP_3]$ does not necessitate a higher $[Ca^{2+}]_i$ to inhibit the channel. Indeed, the P_o of $InsP_3R$-1 is equally low at 60 μM $[Ca^{2+}]_i$ in the presence of 180 μM or 10 μM $InsP_3$ (Mak et al., 1998).

(vi) The maximum channel P_o (P_{max}) attained when the $InsP_3R$ is optimally activated is ∼0.8, less than 1 (Mak et al., 1998, 2001b).

(vii) The regulation of the $InsP_3R$ channel P_o by Ca^{2+} and $InsP_3$ mainly affects the mean closed channel duration $\langle\tau_c\rangle$, which correlates inversely with the channel P_o, decreasing when the channel is activated and increasing when the channel is inhibited (Mak et al., 1998, 2001b,c). On the other hand, $\langle\tau_o\rangle$ remains within a narrow range (5–15 ms) over all $[Ca^{2+}]_i$ and $[InsP_3]$ until the channel P_o drops to <0.1 (Mak et al., 1998, 2001b,c).

(viii) In addition to the observed properties of the ligand regulation of single-channel $InsP_3R$ activity, a molecular model of the regulation of the $InsP_3R$ channel must also take into consideration the molecular structure of the channel. It is well established that a functional $InsP_3R$ channel is a tetrameric unit (Mikoshiba et al., 1993). Although different isoforms of $InsP_3R$ can assemble to form heterotetramers (Joseph et al., 1995), the $InsP_3R$ channels (both types 1 and 3 isoforms) studied in our nuclear patch clamp experiments were overwhelmingly homotetrameric (Mak and Foskett, 1994; Mak et al., 2000), made up of four identical $InsP_3R$ molecules. Thus, the molecular model for $InsP_3R$ channel should exhibit either a fourfold sym-

metry or a twofold symmetry (dimer of dimers: Liu et al., 1998; Richards and Gordon, 2000).

(ix) Biochemically, multiple (>3) Ca^{2+}-binding regions in the $InsP_3R$ sequences have been identified experimentally (Sienaert et al., 1996, 1997). These sequences, which are located mostly on the cytoplasmic side of the $InsP_3R$ molecule with one exposed to the lumen of the ER, may regulate $InsP_3R$ channel activities. In contrast, only one $InsP_3$-binding region has been identified in the $InsP_3R$ sequence (Yoshikawa et al., 1996).

Allosteric Models Considered for Describing the Ligand Regulation of the $InsP_3R$ Channel

Because previously proposed models of $InsP_3R$ gating, in which only the $InsP_3$-bound state(s) of the receptor can be active, fail to account for the spontaneous, $InsP_3$-independent channel activities of the $InsP_3R$, we systematically examined a series of allosteric models in increasing levels of complexity to find the simplest molecular model that can account for all the characteristics of the regulation by $[InsP_3]$ and $[Ca^{2+}]_i$ of the $InsP_3R$ channel tabulated in the previous section. We started with allosteric schemes based on the Monod-Wyman-Changeux (MWC) model. As outlined in (Monod et al., 1965), the four identical $InsP_3R$ molecules in the homotetrameric channel occupy equivalent positions (condition viii) with an axis of rotational symmetry along the axis of the pore of the channel (as depicted in Mikoshiba et al., 1993), and the four monomers in the channel always adopt the same conformation, changing from one conformation to another concertedly. The $InsP_3R$ channel can change from one conformation with any number of ligands bound to its ligand-binding sites to another conformation with the same number of ligands bound. The equivalent ligand-binding sites of all the identical monomers in an $InsP_3R$ channel have the same affinity. Furthermore, whereas the affinities of the ligand-binding sites can differ in different conformations of the channel, they are not affected by the state of occupation of any other ligand-binding site (Monod et al., 1965; Changeux and Edelstein, 1998). The following MWC-based models were examined:

(a) MWC models in which the $InsP_3R$ tetramer can assume two conformations (one open and one closed), and each $InsP_3R$ monomer has two or more Ca^{2+}-binding sties (at least one activating and one inhibitory);

(b) MWC-based models in which the $InsP_3R$ tetramer has three conformations (one open and two closed conformations, or two open and one closed conformations), and each $InsP_3R$ monomer has two Ca^{2+}-binding sites;

(c) an MWC-based model in which the $InsP_3R$ tetramer has four conformations (two open and two closed conformations), and each $InsP_3R$ monomer has two Ca^{2+}-binding sites;

(d) an MWC-based model in which the $InsP_3R$ tetramer has four conformations (two open and two closed conformations), and each $InsP_3R$ monomer has three Ca^{2+}-binding sites;

(e) a variation of model (d) in which the $InsP_3R$ tetramer has two extra closed conformations.

Besides MWC-based models, we also examined allosteric models in which the constraints assumed in the MWC-based models were relaxed to various extents to allow more degrees of freedom to describe the gating behaviors of the $InsP_3R$ channel. In those non-MWC models we considered, the constraint that all the $InsP_3R$ monomers in the tetrameric channel change conformation concertedly is retained. However, the constraints that the equivalent ligand-binding sites of all the monomers in an $InsP_3R$ channel have the same affinity, and that the affinities of the ligand-binding sites are not affected by the state of occupation of any other ligand-binding site, are selectively relaxed. We examined the following non-MWC models:

(f) a "type I" non-MWC model—an allosteric model in which the affinity of the inhibitory Ca^{2+}-binding site is affected by the binding status of the $InsP_3$-binding site on the same $InsP_3R$ monomer—with the $InsP_3R$ tetramer having two conformations, and each $InsP_3R$ monomer having one activating Ca^{2+}-binding site and one inhibitory Ca^{2+}-binding site;

(g) a type I non-MWC model with the $InsP_3R$ tetramer having two conformations, and each $InsP_3R$ monomer having one activating and two inhibitory Ca^{2+}-binding sites, with only one of the inhibitory Ca^{2+}-binding sites affected by $InsP_3$ binding;

(h) a "type II" non-MWC model—an allosteric model in which $InsP_3$ binding to the $InsP_3$-binding sites in the tetramer affects the affinities of all the inhibitory Ca^{2+}-binding sites and $InsP_3$-binding sites in the tetramer—with the $InsP_3R$ tetramer having two conformations, and each $InsP_3R$ monomer having one activating and one inhibitory Ca^{2+}-binding sites;

(i) a type II non-MWC model with the $InsP_3R$ tetramer having two conformations, and each $InsP_3R$ monomer having one activating and two inhibitory Ca^{2+}-binding sites;

(j) a variation of model (i) in which the $InsP_3R$ tetramer has three conformations.

In all the models considered, each $InsP_3R$ monomer has only one $InsP_3$-binding site because of condition (ix). Detailed descriptions of all the models considered, mathematical derivation of analytical formulas to calculate the $InsP_3R$ channel P_o at various $[InsP_3]$ and $[Ca^{2+}]_i$, the rationales for selecting those models to be studied and not considering other possible allosteric models, and comparisons of experimental $InsP_3R$ chan-

nel P_o with those calculated according to the various models, are provided in either the APPENDIX (model (e)), or the online supplemental material section (all other models) available at http://www.jgp.org/cgi/content/full/jgp.200308809/DC1.

Basic Features of the Simplest Allosteric Model That Can Describe the Ligand Regulation of $InsP_3R$ Channel Activity

Among all the models considered, the simplest model, defined as the one involving the fewest number of free parameters (Jones, 1999), that can account for all our observations of the regulation by $[Ca^{2+}]_i$ and $[InsP_3]$ of $InsP_3R$ channel activity, and can satisfy the constraints imposed by the structure of the $InsP_3R$ channel, is the MWC-based, four-plus-two-conformation model (model e above). This model postulates that the $InsP_3R$ monomers, and therefore the $InsP_3R$ tetrameric channel as a whole, can adopt six different conformations (Fig. 7). The channel is open when it is in the A* and C* conformations. The B, D, A′, and C′ conformations are closed. The equilibria between A*, B, C*, and D conformations are dependent on $InsP_3$ and Ca^{2+} binding to the channel, which confers regulation of channel activity by $[InsP_3]$ and $[Ca^{2+}]_i$. In contrast, the equilibrium A*↔A′ is not affected by $[InsP_3]$ or $[Ca^{2+}]_i$, i.e., the affinities of the $InsP_3$ and Ca^{2+} sites of the $InsP_3R$ channel are the same in A* and A′. The ratio of the total durations an $InsP_3R$ channel spends in the A* conformation and in the A′ conformation is the same regardless of $[InsP_3]$ and $[Ca^{2+}]_i$. Thus, the A* and A′ conformations can be grouped together as the "active" A conformation (a conformation in which the channel can open, denoted by a green box in Fig. 7) when we consider the effects of $InsP_3$ and Ca^{2+} on channel conformations. Similarly, C′ and C* are grouped together as the active C conformation (denoted by a green box with dashed border in Fig. 7) because the equilibrium C*↔C′ is likewise not affected by $[InsP_3]$ or $[Ca^{2+}]_i$. Thus, even in the presence of optimal $[InsP_3]$ and $[Ca^{2+}]_i$, when the $InsP_3R$ channel hardly exists in the closed B and D conformations, the maximum observed channel P_o is <1 because the channel exists a fraction of the time in the closed A′ and C′ conformations. This accounts for the observation that the maximum $InsP_3R$ channel P_o in saturating $[InsP_3]$ (10 μM) and optimal $[Ca^{2+}]_i$ is only ~0.8 (<1) (Mak et al., 1998). The model also postulates that each of the four $InsP_3R$ monomers has one $InsP_3$-binding site (Q) and three different functional Ca^{2+}-binding sites (F, G, and H) on the cytoplasmic side of the channel. Because of its tetrameric structure, an $InsP_3R$ channel can bind a maximum of four $InsP_3$ molecules in its Q sites and four Ca^{2+} in each of the three types (F, G, and H) of Ca^{2+} sites. The affinities of these ligand-binding sites are different in the different channel conformations (A, B, C, and D). $InsP_3$ and Ca^{2+} regulate channel activity because binding of $InsP_3$ or Ca^{2+} to these sites will stabilize those conformations in which the sites have higher affinities, thereby affecting the equilibria among the A, B, C, and D conformations, as outlined in Monod et al. (1965).

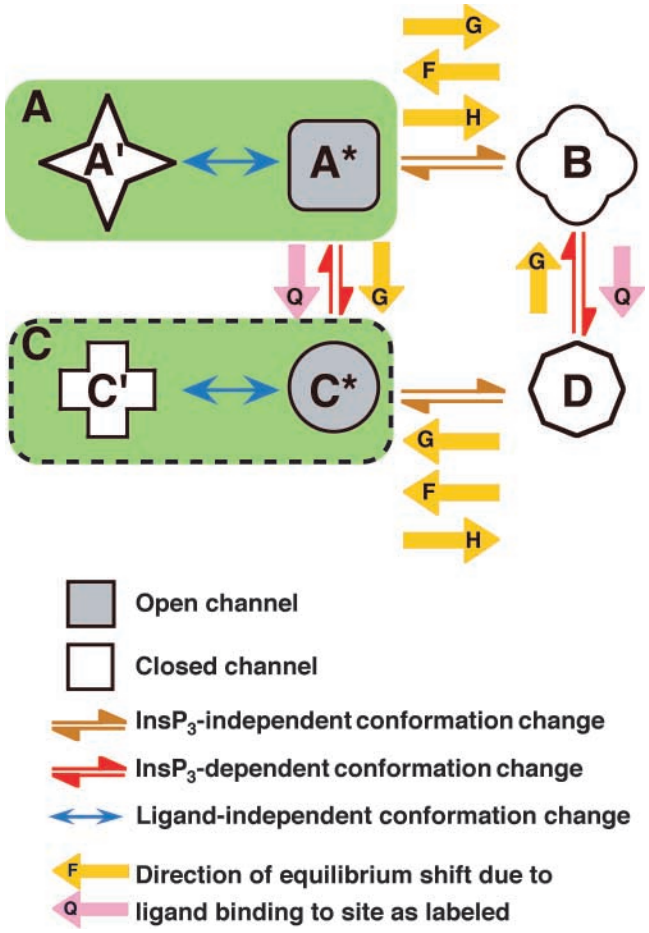

FIGURE 7. The MWC-based four-plus-two-conformation model for $InsP_3R$ channel gating. Only conformation transitions are represented in the schemes. Reactions involving binding of $InsP_3$ and Ca^{2+} to the $InsP_3R$ channel and the state of occupation of the various ligand-binding sites of the channel are omitted from the schemes for clarity. The green boxes represent the grouping of the open A* and closed A′ conformations into the active A conformation, and the grouping of the C* and C′ conformations into the active C conformation.

An important feature of a MWC-based model of ligand regulation is that the effect of ligand binding on the equilibrium between two channel conformations is determined by the affinities of the site in the two conformations. At ligand concentrations << the lower dissociation constant of the site, there is not enough ligand binding to the site to shift the equilibrium position. At ligand concentrations >> the higher dissociation constant, the ligand binding site is saturated and

ligand concentration is no longer relevant to the equilibrium position since the ligand will bind to the site regardless of what conformation the channel is in. Thus, the difference between the higher and lower dissociation constants of the site corresponds approximately to the range of ligand concentrations over which the effects of the site can be felt. Importantly, the magnitude of the difference between the two affinities of the site determines the full extent of the effect of the site, i.e., how much activation or inhibition the site produces between zero and saturating ligand concentrations. (Of course, this cannot be the case if the difference between the dissociation constants is so large that the equilibrium position is already totally shifted to the favorable conformation before the ligand concentration becomes >> higher dissociation constant.)

The mechanisms for Ca^{2+} and $InsP_3$ regulation are mostly segregated in this model (see the APPENDIX for more detailed reasoning behind this assertion), allowing further reduction in the number of free parameters involved. This means that in our model, $InsP_3$ binding to the Q sites only affects the equilibria A↔C, and B↔D (red double arrows in Fig. 7). In the absence of $InsP_3$, the equilibria overwhelmingly favor the A and B conformations. $InsP_3$ regulates the $InsP_3R$ channel solely by stabilizing the C conformation relative to the A conformation; and stabilizing the D conformation relative to the B conformation (indicated by the pink arrows in Fig. 7). Thus, in saturating [$InsP_3$], the channel exists mostly in the C and D conformations. The equilibria A↔B and C↔D (brown double arrows in Fig. 7) are $InsP_3$-independent, i.e., the affinities of the Q sites in A and B conformations are the same, and so are those of the Q sites in C and D conformations.

The F sites are responsible for the $InsP_3$-independent Ca^{2+} activation of the channel. Ca^{2+} binding to the F sites only affects the $InsP_3$-independent A↔B and C↔D equilibria (brown double arrows in Fig. 7), stabilizing the active A and C conformations (indicated by the yellow arrows in Fig. 7). The affinities of the F sites are the same in A and C conformations, and so are the affinities of those in B and D conformations. Thus, Ca^{2+} binding to the F sites does not affect the $InsP_3$-dependent A↔C, or B↔D equilibria (red double arrows in Fig. 7).

The H sites are responsible for inhibition of the channel by high $[Ca^{2+}]_i$. The affinities of the H sites are the same in the A and C conformations and are the same in the B and D conformations. Thus, $InsP_3$-induced shifts (pink arrows in Fig. 7) in the A↔C and B↔D equilibria (red double arrows in Fig. 7) do not affect Ca^{2+} binding to the H sites. Ca^{2+} binding to the H sites only affects the $InsP_3$-independent equilibria A↔B and C↔D (brown double arrows in Fig. 7), stabilizing the closed B and D conformations relative to the active A and C conformations (indicated by the yellow arrows).

TABLE I

Parameters Used to Calculate the P_o for $InsP_3R$-1 and $InsP_3R$-3 in Fig. 8 According to the MWC-based Four-Plus-Two-Conformation Model with Three Ca^{2+}-binding Sites per $InsP_3R$ Monomer

Parameters	$InsP_3R$-1[a]	$InsP_3R$-3
L_{BA}	29.2	38.7
L_{DB}	2.50×10^{-5}	0.412
L_{CA}	1.86×10^{-5}	9.12×10^{-3}
$K^{FA} = K^{FC} = K^{F1}$	223 nM	1.01 nM
$K^{FB} = K^{FD} = K^{F2}$	271 nM	5.47 nM
K^{GA}	>200 nM[b]	>100 nM[b]
K^{GB}	58.63 nM	2.69 nM
K^{GC}	153 nM	261 nM
K^{GD}	1.37 μM	661 nM
$K^{HA} = K^{HC} = K^{H1}$	>1 mM[b]	>1 mM[b]
$K^{HB} = K^{HD} = K^{H2}$	19 μM	32 μM
$K^{QA} = K^{QB} = K^{Q1}$	>3 μM[b]	>3 μM[b]
$K^{QC} = K^{QD} = K^{Q2}$	0.28 nM	0.30 nM
$R = [A^*]/[A'] = [C^*]/[C']$	5.74	8.31

It should be noted that although the calculated channel P_o derived from these sets of parameters agree reasonably well with experimental data, these sets of parameters may not be unique. Other sets of parameters that give good fits may exist in the huge parameter space.

[a]The same set of parameters can be used to fit *X*-$InsP_3R$-1 channel P_o in ultra-low bath $[Ca^{2+}]$ except $K^{H1} = K^{H2}$. As long as $K^{H1} = K^{H2}$, Ca^{2+} binding to H sites will not stabilize one conformation relative to another and the H sites will no longer be functional.

[b]These parameters can only be determined to be greater than the tabulated values because the calculated P_o are not very sensitive to these parameters.

Regulation of the $InsP_3R$ by the G sites is more complex because the G sites have different affinities (Table I) in the four conformations (A, B, C, and D). The G sites in the closed B conformation have higher Ca^{2+} affinity than those in the active A conformation, so that the G sites are inhibitory Ca^{2+}-binding sites (as indicated by the top yellow arrow in Fig. 7) in the A↔B equilibrium, which is the dominating equilibrium in the absence of $InsP_3$. Most interestingly, however, the G sites in the active C conformation have higher Ca^{2+} affinity than those in the closed D conformation, so in the C↔D equilibrium, which is the dominating equilibrium under saturating [$InsP_3$], the G sites are activating Ca^{2+}-binding sites (as indicated by the yellow arrow in the lower half of Fig. 7). Between zero and saturating [$InsP_3$], $InsP_3$ binding to the channel shifts it from the A and B conformations toward the C and D channel. Thus, in subsaturating [$InsP_3$], the "effective" dissociation constant of the G sites in the closed channel lies between those in the B and D conformations, according to the equilibrium position of the channel among the conformations as dictated by [$InsP_3$]. Similarly, the "effective" dissociation constant of the G sites in the active conformations lies between those in the A and C

conformations. As [$InsP_3$] increases, not only do the G sites change from being inhibitory to activating, the difference between the effective affinities of the G sites in the closed and active channel also changes. As discussed earlier, the $InsP_3$-induced change in the magnitude of the affinity difference of the G sites alters the full extent of the effect of the G sites on the channel, i.e., how much activation (or inhibition) the G sites produce between zero and saturating $[Ca^{2+}]_i$. It should be noted that since the F and H sites are both $InsP_3$ independent, the G site is the only one modulated by $InsP_3$ binding to the channel. Thus, all $InsP_3$ regulation of the $InsP_3R$ stems from the effect of $InsP_3$ binding on the properties of the G site.

Since $InsP_3$ binding to the channel affects Ca^{2+} binding to G sites, microreversibility dictates that Ca^{2+} binding to G sites should affect the $InsP_3$-dependent equilibria A↔C and B↔D (as indicated by the vertical yellow arrows in Fig. 7). However, this effect is much weaker than the effect of $InsP_3$ binding to the Q sites and so is not noticeable in our experiments.

Considering the $InsP_3$-independent equilibria A↔B and C↔D, the affinities of the Ca^{2+}-binding sites are in the order G ∼ F > H. For the C↔D equilibrium, Ca^{2+} will tend to bind first to the G sites and the F sites, both stabilizing the open C conformation, and then to the H sites, stabilizing the closed D conformation. For the A↔B equilibrium, as $[Ca^{2+}]_i$ increases, Ca^{2+} will tend to first bind to the G sites, stabilizing the closed B conformation, and to the F sites, stabilizing the open A conformation. However, Ca^{2+} binding to the F sites cannot overcome the inhibitory effects of the G sites, so the channel remains mostly in the closed conformation. This is because the magnitude of the difference between the affinities of the G site in the closed B and active A conformations is greater than that of the F sites (Table I). Thus, the F site is less effective at activating the channel than the G site is at inhibiting it.

It should be noted that this molecular model does not take into consideration the kinetically abrupt termination of the $InsP_3R$ channel activities that causes the channel activities observed in our patch clamp experiments to disappear over time under constant [$InsP_3$] and $[Ca^{2+}]_i$ (Mak and Foskett, 1997). Therefore, it also does not account for any possible Ca^{2+} dependence of the termination of the channel activities (Boehning et al., 2001). Furthermore, this model does not consider other ligands that bind at or near the $InsP_3$ binding site and activate channel gating, including the fungal metabolite adenophostin (Takahashi et al., 1994; Marchant et al., 1997; Mak et al., 2001c) and the neuronal CaBP1 protein (Yang et al., 2002). We have restricted our analyses to $InsP_3$ because the dataset is much more extensive. To a first approximation, however, we believe that our conclusions regarding the effects of $InsP_3$ can likely be generalized to these other ligands as well.

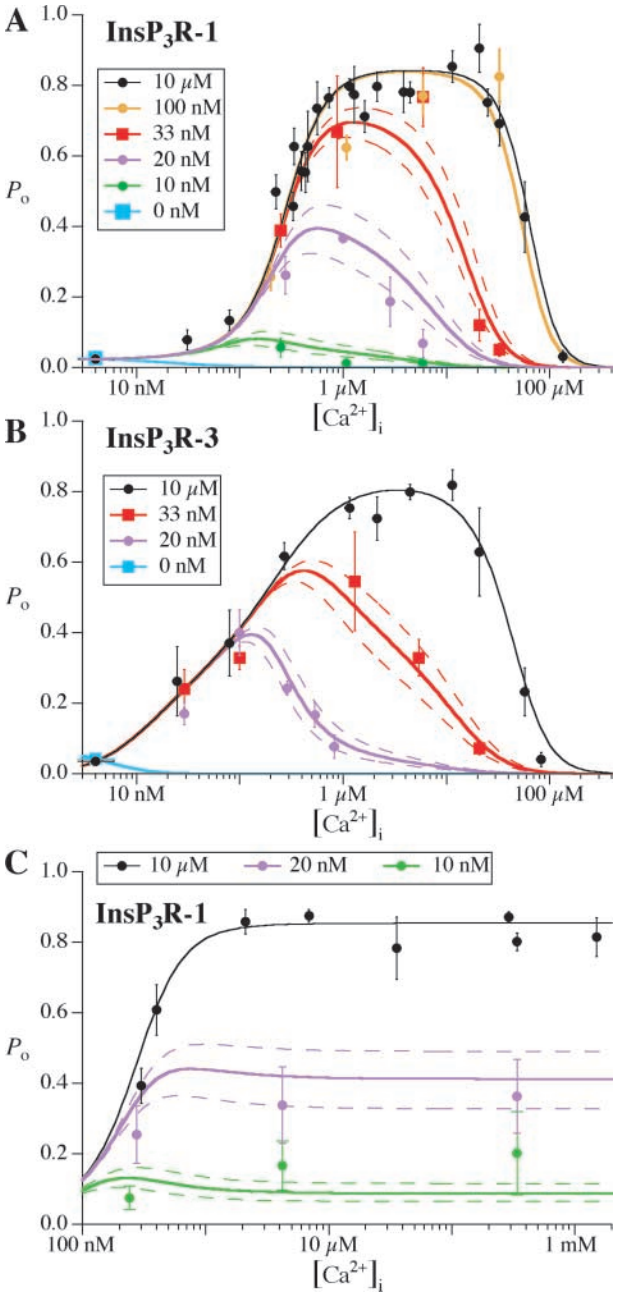

FIGURE 8. Fitting of the $InsP_3R$ channel P_o in various $[Ca^{2+}]_i$ and [$InsP_3$] by the MWC-based four-plus-two-conformation model. (A) $InsP_3R$-1 in regular bath (300 nM $[Ca^{2+}]$), (B) $InsP_3R$-3 in regular bath (300 nM $[Ca^{2+}]$), and (C) $InsP_3R$-1 in bath containing <5 nM Ca^{2+}. The symbols represent the experimental P_o in the tabulated [$InsP_3$]. The continuous curves are the theoretical P_o calculated from the model. The dashed curves indicate the range of calculated P_o for ± 10% of the tabulated [$InsP_3$]. Parameters used for the P_o calculations are tabulated in Table I.

Agreement between the Selected Simplest Allosteric Model and Features of $InsP_3$ and Ca^{2+} Regulation of $InsP_3R$ Channel Observed in Regular Bath Solution

We extended the mathematical treatment for the MWC allosteric model outlined in (Monod et al., 1965) to de-

rive analytical equations to evaluate the channel P_o in the presence of various [$InsP_3$] and [Ca^{2+}]$_i$ according to the MWC-based four-plus-two-conformation model (see APPENDIX for derivation of the equations). The theoretical channel P_o values calculated from these equations (Fig. 8) with the optimized set of physical parameters (dissociation constants of the various ligand-binding sites in different channel conformations, and the equilibrium constants of the transitions between different channel conformations in the absence of any ligands, as listed in Table I) fit reasonably well the experimental channel P_o observed in extensive nuclear patch-clamp studies for both types 1 and 3 isoforms (Mak et al., 1998, 2001b, 2003; and this study).

It should be noted that the agreement between theoretical and experimental channel P_o is remarkable considering the multitude of distinctive features of ligand regulation of $InsP_3R$ channel activities the model had to account for, and the wide range of [$InsP_3$] and [Ca^{2+}]$_i$ examined for two distinct channel isoforms from two species.

Specifically, the model accounts for the following experimentally observed features.

The $InsP_3R$ Channel Can Be Active When None of its Ligand Binding Sites Is Occupied (Condition i)

The spontaneous $InsP_3R$ channel activities observed in this study are accounted for in the model as they are in the standard MWC model. In the absence of any ligand binding ([Ca^{2+}]$_i$ $<$ 5 nM and 0 $InsP_3$), the channel is mostly in the closed B conformation. However, there is a nonzero probability for the channel to adopt the open A* conformation, giving rise to the spontaneous channel activities observed.

Why does raising the [Ca^{2+}]$_i$ inhibit spontaneous opening? In the absence of $InsP_3$, the channel exists overwhelmingly in the A and B conformations. In these conformations the Ca^{2+}-binding G sites are inhibitory and they are more effective than the activating Ca^{2+}-binding F sites, as discussed above. Therefore, no channel activity is observed at [Ca^{2+}]$_i$ = 25 nM because, at that concentration, cytoplasmic Ca^{2+} will bind to the G sites and stabilize the closed B conformation strongly, thus inhibiting channel activity. Ca^{2+} binding to the activating F sites also occurs, but F site occupancy is insufficient to counter the inhibitory effect of the G sites.

$InsP_3$ has No Effect on Ca^{2+} Activation Parameters (K_{act} and H_{act}) of the $InsP_3R$ Channel (Condition ii)

In our model, Ca^{2+} binding to the F sites activates the $InsP_3R$ channel by stabilizing the active A and C conformations relative to the closed B and D conformations. [$InsP_3$] has no effect on this Ca^{2+} activation of channel activity because:

(1) the A↔B and C↔D (active↔closed) equilibria (brown double arrows in Fig. 7) that are driven by Ca^{2+} binding are $InsP_3$ independent; and

(2) in the $InsP_3$-dependent A↔C and B↔D equilibria (red double arrows in Fig. 7), Ca^{2+} affinities of the F sites are not affected by [$InsP_3$] because the affinities of F sites are the same in the A and C conformations, and also the same in the B and D conformations (Table I).

Nevertheless, a novel insight emerges from our model: there is another, distinct contribution to Ca^{2+} activation that is indeed provided by $InsP_3$. This $InsP_3$-dependent contribution to the Ca^{2+} activation of the channel arises because $InsP_3$ changes the G sites from inhibitory to activating. However, empirically, this effect is not clearly distinguishable from the activation of the channel by the F sites because of the similar affinities of the activating F and G sites in the C conformation of the $InsP_3R$ channel (i.e., $K^{FC} \approx K^{GC}$ in Table I). This can account for why just one set of Ca^{2+} activation parameters (K_{act} and H_{act}) in the empirical Hill equation was required to fit the experimental observations, and why those parameters exhibited no $InsP_3$ dependence (Mak et al., 1998, 2001b).

Biphasic [Ca^{2+}]$_i$ Regulation of $InsP_3R$ Channel Activity Is Observed at all [$InsP_3$] (Condition iii)

A distinguishing feature of our allosteric model is that a third type of Ca^{2+}-binding site, the H site, is postulated to exist. Besides the $InsP_3$-independent activating F sites, and the G sites that are entirely responsible for the $InsP_3$ dependence of the channel, inclusion of this novel $InsP_3$-insensitive inhibitory site in the model was necessary to account for Ca^{2+} inhibition of the channel. The H sites are independent of [$InsP_3$] because their affinities are the same in the B and D channel conformations, and in the A and C conformations (Table I).

In low [$InsP_3$] at which the G sites are inhibitory, the activating F sites and the inhibitory G sites together produce the biphasic Ca^{2+} regulation observed. The inhibitory effect of the H sites is not observable. As [$InsP_3$] increases, the G sites become activating. Then the $InsP_3$-independent H sites are the only inhibitory Ca^{2+}-binding sites. The activating F and G sites, together with the inhibitory H sites, produce the biphasic Ca^{2+}dependence of the channel P_o. Thus, the biphasic Ca^{2+} regulation is observed at all [$InsP_3$].

Ca^{2+} Inhibition of $InsP_3R$ Channel Activity Is Sensitive to Small Changes in [$InsP_3$] (Condition iv)

Several factors contribute to the exquisite sensitivity of the channel P_o to small changes in [$InsP_3$] at low [$InsP_3$]. The affinity of the Q sites for $InsP_3$ in the C and D channel conformations is extremely high (Table I) so that even at very low concentrations, $InsP_3$ starts to

bind to the channel. Furthermore, as [$InsP_3$] increases, the strong binding of $InsP_3$ to the Q sites rapidly shifts the equilibrium toward the C and D conformations. As discussed above, this shift changes the effective affinities of the G sites in the closed and active channel, thereby changing the nature of the G sites from inhibitory to activating. Consequently, the mechanism of Ca^{2+} inhibition of the channel changes from being mediated by Ca^{2+} binding to the high-affinity G sites to being mediated by Ca^{2+} binding to the low-affinity H sites. This switch results in a substantial change in the ability of Ca^{2+} to inhibit the channel. Consequently, the apparent half-maximal inhibitory $[Ca^{2+}]_i$ (K_{inh}) of the type 1 $InsP_3R$ changes >300-fold when [$InsP_3$] increases just 10-fold (Mak et al., 1998), even though each $InsP_3R$ monomer has only one $InsP_3$-binding site.

Response of $InsP_3R$ to $InsP_3$ Saturates Rapidly and Abruptly by [$InsP_3$] = 100 nM so That Higher [$InsP_3$] Does Not Require Higher $[Ca^{2+}]_i$ for Inhibition (Condition v)

The abrupt saturation of the response of the $InsP_3R$ to $InsP_3$ cannot be due to saturation of the $InsP_3$ binding site because the apparent affinity of Ca^{2+} to inhibit the type 1 $InsP_3R$ channel (K_{inh}) is still highly sensitive to changes in [$InsP_3$] near 100 nM where the response saturates. The G sites are activating at 100 nM $InsP_3$, so the only mechanism available for Ca^{2+} inhibition of the channel is that mediated by Ca^{2+} binding to the H sites. The abrupt saturation of the response to $InsP_3$ is due to the fact that properties of the H sites are $InsP_3$ independent. Even as [$InsP_3$] is further increased over three orders of magnitude, the same $[Ca^{2+}]_i$ is required to inhibit the $InsP_3R$ channel (Mak et al., 1998).

The Maximum Channel P_o Is Always ~0.8 (Condition vi)

Even when the experimental conditions are optimized to bias the equilibria among the A, B, C, and D channel conformations in favor of the active conformations, the observed channel P_o is still limited by the fact that the $InsP_3R$ channel in the active A (or C) conformation spends only a fraction of its time being open (in the A* or C* conformation), resulting in channel $P_{max} < 1$. Furthermore, because the ligand-independent equilibria A*↔A′ and C*↔C′ have the same equilibrium constant in our model, the theoretical channel P_{max} is not affected by any of the experimental conditions that may shift the equilibria among the A, B, C, and D conformations. This feature accounts for the observation that the channel P_{max} remains the same in all experiments. It is possible that the ligand-independent conformation transitions A*↔A′ and C*↔C′ are controlled by a gating mechanism different from that controlling the ligand-dependent conformation transitions among A*, C*, B, and D.

The Mean Channel Open Duration $<\tau_o>$ Is Ligand Independent over a Wide Range of $[Ca^{2+}]_i$ and [$InsP_3$], Whereas the Mean Channel Closed Duration Is Ligand Dependent (Condition vii)

According to the model, an open channel in the A* or C* conformations can close either through a ligand-dependent transition into the B or D conformations, or through a ligand-independent transition into the A′ or C′ conformations (Fig. 7). The observed mean channel open duration $<\tau_o>$ is determined by the fastest one of the transitions out of the open A* and C* conformations. Our model postulates that the rates of the ligand-independent conformation transitions, A*↔A′ and C*↔C′, are substantially higher than the rates of the ligand-dependent transitions among the A*, C*, B, and D conformations under most [$InsP_3$] and $[Ca^{2+}]_i$ examined. Thus, once the channel opens into the A* (or C*) conformation from the B (or D) conformation, it undergoes many ligand-independent A*↔A′ (or C*↔C′) transitions before it closes via a ligand-dependent transition back to the B or D conformations. This limits the open channel duration. The rates of channel closing via the ligand-dependent transitions (A*→B, A*→D, C*→B and C*→D) become comparable to the ligand-independent transitions (A*→A′ and C*→C′) only in conditions ($[Ca^{2+}]_i << K_{act}$, or $[Ca^{2+}]_i >> K_{inh}$) when channel activity is significantly inhibited ($P_o < 0.1$). Therefore, the observed $<\tau_o>$ of $InsP_3R$ channel remain within a narrow range even under various conditions of $[Ca^{2+}]_i$ and [$InsP_3$] in which the channel P_o changes dramatically (Mak et al., 1998, 2001b,c). $<\tau_o>$ only decreases when channel activity is substantially inhibited ($P_o < 0.1$), when one of the ligand-dependent channel-closing transitions becomes more frequent than the ligand-independent transitions.

We rejected the possibility that the channel conformations are connected such that A*↔A′↔B because in this case, the channel can only exit the open A* and C* conformations by entering the closed A′ and C′ conformations, respectively, through ligand-independent conformation transitions. In that case, $<\tau_o>$ would not be affected by $[Ca^{2+}]_i$ or [$InsP_3$] at all, contrary to observations.

On the other hand, a closed channel in the B and D conformations opens only through ligand-dependent transitions, whereas a closed channel in the A′ and C′ conformations opens only through ligand-independent transitions. The mean channel closed duration $<\tau_c>$, the mean of the durations of the channel being in the B, D, A′, and C′ conformations, is dominated by the slowest of the channel opening transition rates, which is ligand dependent in our model. Hence, $<\tau_c>$ exhibits ligand dependence with a trend opposite to that of the channel P_o, i.e., $<\tau_c>$ decreases as channel P_o increases

and vice versa, as observed in our experiments (Mak et al., 1998, 2001b).

Ligand Regulation of the $InsP_3R$ Channel after Exposure to Ultra-low Bath [Ca^{2+}] Can be Accounted for by the MWC-based Four-Plus-Two-Conformation Allosteric Model

The MWC-based four-plus-two-conformation allosteric model postulates that the $InsP_3R$ channel has three types of regulatory Ca^{2+}-binding sites that are mutually independent. The model predicts, therefore, that it could be theoretically possible, by mutagenesis or other experimental or physiological means, to specifically modify any one of the Ca^{2+}-binding sites without affecting the other ligand binding sites. Furthermore, the model enables quantitative predictions to be made about the behavior of a channel with any specific Ca^{2+} site so modified. We therefore considered whether the novel $InsP_3R$-1 channel behaviors observed following exposure of nuclei to an ultra-low bath [Ca^{2+}] (Mak et al., 2003) could be predicted from our model by assuming that the experimental treatment specifically rendered the H site nonfunctional, because this site is responsible for high Ca^{2+} inhibition. In other words, we simply assumed that the only effect of exposure to ultra-low bath [Ca^{2+}] is to make the affinities of the H sites the same in the A, B, C, and D conformations. Remarkably, the observed channel behaviors are well-predicted by this assumption.

First, with the inhibitory H sites rendered nonfunctional by exposure to ultra-low bath [Ca^{2+}], the model predicts that the channel will exhibit no Ca^{2+} inhibition in [$InsP_3$] that is high enough ($\geq$10 nM), such that the combined effect of Ca^{2+} binding to the F and G sites is activating. Indeed, in all [$InsP_3$] used (10 nM, 20 nM, and 10 μM), the channel P_o observed in our experiments after the nuclei were exposed to ultra-low bath [Ca^{2+}] increased as $[Ca^{2+}]_i$ was raised from 100 nM to 2 μM due to the combined activating effect of the F and G sites. Then the channel P_o remained at the same plateau value for all $[Ca^{2+}]_i > 2$ μM (up to 1.5 mM) with no detectable inhibition by $[Ca^{2+}]_i$ (Mak et al., 2003). The model predicts this because with the F and G sites being activating and no functional H sites, there is no more Ca^{2+}-binding sites in the $InsP_3R$ channel to generate any inhibitory effect.

Second, the model predicts that rendering the H sites nonfunctional by exposure to ultra-low bath [Ca^{2+}] should not affect the function of the F and G sites because the Ca^{2+}-binding sites are independent in our model. Thus, the model predicts that exposure to ultra-low bath [Ca^{2+}] should have no effect on the Ca^{2+} activation properties of the channel in saturating [$InsP_3$]. Indeed, in 10 μM [$InsP_3$], Ca^{2+} activation (100 nM $< [Ca^{2+}]_i <$ 1 μM) of the channel exposed to ultra-low bath [Ca^{2+}] was very similar to that of channels exposed to regular bath [Ca^{2+}] (400–500 nM) (Mak et al., 2003).

Third, the model predicts that even with the H sites nonfunctional, the $InsP_3R$ channel activity should nevertheless remain $InsP_3$ dependent because the G sites remain inhibitory in the absence of $InsP_3$. This is indeed what was observed. Even though the major apparent effect of $InsP_3$ is to relieve high $[Ca^{2+}]_i$ inhibition of the channel exposed to regular bath [Ca^{2+}] (Mak et al., 1998), and exposure of the channel to the ultra-low bath [Ca^{2+}] eliminates high $[Ca^{2+}]_i$ inhibition in the presence of saturating $InsP_3$, $InsP_3$ nevertheless is still required to activate channel activity (Mak et al., 2003).

Fourth, the model predicts that even with the H site nonfunctional, and with the experimental conditions overwhelmingly favoring the channel being in the active C conformation, the channel will still exist for a ligand-independent fraction of time in the closed C′ conformation. Indeed, even after exposure to ultra-low bath [Ca^{2+}], the channel still exhibited a P_{max} of $\sim$0.8, ($<$1) in saturating [$InsP_3$] and high $[Ca^{2+}]_i$ (Mak et al., 2003).

More importantly, the model predicts that distinct and novel channel behavior should be observed in subsaturating [$InsP_3$] after exposure to an ultra-low bath [Ca^{2+}] renders the H sites nonfunctional. Specifically, in the absence of functional H sites, the model indicates that the effect of $InsP_3$ on the channel should be manifested as a change in the maximum channel P_o, a behavior distinguished from the behavior of the channel with the H site functional, where the effect of $InsP_3$ is manifested as a change in the apparent K_{inh}, with no effect on the parameter P_{max} used in the biphasic Hill equation (Eq. 1). The observed behavior of the channel in various [$InsP_3$] after exposure to an ultra-low bath [Ca^{2+}] (Mak et al., 2003) is in very good agreement with this prediction. Understanding this novel behavior requires consideration of the effects of $InsP_3$ on the properties of the G site. In subsaturating [$InsP_3$], increases in [$InsP_3$] shifts the channel toward the C and D conformations. This not only changes the nature of the G site from being inhibitory to activating, but also changes the difference between the effective affinities of the G site in the closed and active channel, thereby alters how much activation or inhibition the G site produces. At $\sim$10 nM, the equilibria of the *X*-$InsP_3R$-1 is shifted sufficiently toward the C and D conformation that the G sites become activating (Fig. 8). Thus, as $[Ca^{2+}]_i$ increases from 0.1 to 2 μM, Ca^{2+} binding to the F and G sites activates the channel and raises the channel P_o (Fig. 8 C). However, the extent of this activation is limited because at 10 nM [$InsP_3$], the difference between the effective affinities of the G sites in the closed and active channel is small. Thus, the channel P_o is only increased to a maximum of 0.2 (Mak et al., 2003), sub-

stantially lower than $P_{max} \approx 0.8$. With no functional H sites, there is no Ca^{2+} inhibition so the channel P_o remains at that maximum level even as $[Ca^{2+}]_i$ increases. Further increases in $[InsP_3]$ further favor the C and D conformations, increasing the difference between the effective affinities of the G sites, thereby enhancing the extent of activation of the channel. This enhancement is manifested as an increase in the maximum P_o the channel exhibits. Increases in $[InsP_3]$ continue to raise the maximum channel P_o until it reaches 0.8—P_{max}, which is dictated by the C′↔C* equilibrium.

Thus, with a single simple assumption that the exposure of the $InsP_3R$ channel to ultra-low bath $[Ca^{2+}]$ renders the H sites in the channel nonfunctional, the MWC-based, four-plus-two-conformation allosteric model can quantitatively account for the ligand regulation of the channel exposed to ultra-low bath $[Ca^{2+}]$ observed in (Mak et al., 2003), without involving any additional free parameters. This is significant, because the model we have developed here was devised to account for the regulation by $[Ca^{2+}]_i$ and $[InsP_3]$ of the $InsP_3R$ channel in regular bath $[Ca^{2+}]$ (400–500 nM). The fact that it successfully quantitatively predicts independent and distinct experimental data (regulation by $[Ca^{2+}]_i$ and $[InsP_3]$ of the channel after exposure to ultra-low bath $[Ca^{2+}]$) provides strong support for its validity.

We would like to point out that in the extension of our model described above, we use our model to separately account for the behaviors of the $InsP_3R$ channel when it is exposed to regular Ca^{2+} bath, and when it has been exposed to low Ca^{2+} bath. Thus, we limit the description of the sensing mechanism that detects the exposure of the channel to ultra-low bath $[Ca^{2+}]$ to a qualitative one, as a switch that turns on and off the inhibition of channel gating mediated by the H sites, depending on the bath $[Ca^{2+}]$ the channel has been exposed to. We did not attempt to quantitatively incorporate the sensing mechanism into our model for the following reasons. First, our allosteric model is derived based on the behavior of the $InsP_3R$ channel in steady-state conditions. Thus, it cannot, in its present form, provide a quantitative description for the kinetic behavior of $InsP_3R$ channels in response to changes in $[InsP_3]$ and $[Ca^{2+}]_i$, including the time course of the disruption of high-$[Ca^{2+}]_i$ inhibition of the channel after it was exposed to ultra-low bath $[Ca^{2+}]$, or the reversal of the disruption when the nucleus was returned to regular bath $[Ca^{2+}]$. Second, because we do not know the physical location (cytoplasmic or lumenal) of the sensing mechanism in the $InsP_3R$ channel, we cannot be sure of the exact experimental conditions (lumenal or cytoplasmic free $[Ca^{2+}]$) that trigger the disruption of the high $[Ca^{2+}]_i$ inhibition of the channel. Trying to describe this Ca^{2+} sensing mechanism quantitatively will entail developing two alternative models, one for each possible scenario, which is premature at this point. Third, the application of our model to the understanding of the physiological regulation of $InsP_3R$ by $[Ca^{2+}]_i$ and $[InsP_3]$, the main reason for developing the model, is not significantly limited by our qualitative description of the sensing mechanism. This is because at present, disruption of the high $[Ca^{2+}]_i$ inhibition of $InsP_3R$ channels was only observed when the channels were exposed to a very low $[Ca^{2+}]$ (nM), in either cytoplasmic or lumenal sides. Neither of these cases is likely to occur under physiologically relevant situations. The model can be modified later to better incorporate the Ca^{2+} sensing mechanism when further information about the mechanism becomes available, and if physiological conditions are found to disrupt the high $[Ca^{2+}]_i$ inhibition of $InsP_3R$ channel activity.

Conclusions

Examination of $InsP_3R$ channel activity (both *Xenopus* type 1 and rat type 3) in extremely low $[Ca^{2+}]_i$ revealed that $InsP_3$ is not necessary for $InsP_3R$ channel opening. Spontaneous $InsP_3R$ channel activity was observed because the inhibitory Ca^{2+}-binding sites of the channel have a finite affinity even in the absence of $InsP_3$ so that in $[Ca^{2+}]_i < 5$ nM, the inhibitory Ca^{2+}-binding sites are not occupied and there is no Ca^{2+} inhibition of the channel. The observation of spontaneous, ligand-independent activity suggested that the Ca^{2+} and $InsP_3$ regulation of the $InsP_3R$ channel could be described by an allosteric model for channel gating in which a channel that is not bound to Ca^{2+} or $InsP_3$ nevertheless has a finite, nonzero, probability of adopting an open conformation. In contrast, all previous models have assumed that channel opening has a strict requirement for $InsP_3$ binding. Thus, our modeling effort is the first one to incorporate this spontaneous activity into an allosteric model to describe the $InsP_3R$ channel. Furthermore, it is the first quantitative model that takes into consideration the tetrameric structure of the $InsP_3R$ channel, and thus addresses fully and quantitatively the cooperative nature of the activation and inhibition of $InsP_3R$ channel gating by $[Ca^{2+}]_i$, and the cooperative nature of $InsP_3R$ channel regulation by $InsP_3$.

We examined various allosteric models to find one that could describe channel-gating characteristics observed in extensive electrophysiological studies of the $InsP_3R$ in native endoplasmic reticulum membrane. The MWC-based four-plus-two-conformation model with one $InsP_3$- and three different Ca^{2+}-binding sites in each $InsP_3R$ monomer in a tetrameric channel can account for the nine distinct observations that we explicitly defined, including the spontaneous activities observed here, for both the types 1 and 3 $InsP_3R$, over a wide observed range of $[Ca^{2+}]_i$ (~3 nM to 200 μM)

and [$InsP_3$] (0 to 180 μM). This model can account for the experimental observations with the minimum number of free parameters (14), and is therefore considered most likely. Importantly, the model derived from these data can also account for independent observations regarding the lack of Ca^{2+} inhibition (up to 1.5 mM) of channel activity and the $InsP_3$ regulation of the maximum channel P_o exhibited by *X*-$InsP_3R$-1 exposed to ultra-low bath [Ca^{2+}] (< 5 nM) described in the preceding paper (Mak et al., 2003). Of note, it quantitatively did so, and without involving more parameters, by simply assuming that the exposure to ultra-low bath [Ca^{2+}] specifically renders one of the Ca^{2+}-binding sites nonfunctional. The ability of the model to predict this complex behavior strongly validates it, and suggests that it will be useful for interpreting the molecular basis for other channel behaviors observed in future studies.

The model provides insights into the possible molecular mechanisms that enable the $InsP_3R$ channel to be so precisely regulated by $InsP_3$ and Ca^{2+}. It has remained difficult to understand how the $InsP_3R$ channel can be regulated so exquisitely by $InsP_3$. Small changes in [$InsP_3$] over a narrow range (10–100 nM) cause the apparent K_{inh} to change by over 2 orders of magnitude (from 160 nM to 60 μM), even though it is well established that there are only four $InsP_3$-binding sites in each $InsP_3R$ tetrameric channel. Furthermore, the mechanisms that can account for the total saturation of the channel response to [$InsP_3$] once [$InsP_3$] goes beyond 100 nM have also been unclear. Insights into these properties of $InsP_3R$ regulation are highly relevant for understanding the mechanisms that generate rapid and well-controlled Ca^{2+} signals in cells. These properties can now be accounted for in our model, by positing three different functional Ca^{2+}-binding sites in each $InsP_3R$ monomer that directly affect the equilibria among active and closed conformations of the channel. One of these sites is activating, whereas another is inhibitory, but both are independent of $InsP_3$. In contrast, a third Ca^{2+}-binding site is affected by $InsP_3$, being inhibitory in the absence of $InsP_3$ but becoming activating as [$InsP_3$] increases. All previous models of Ca^{2+} regulation of $InsP_3R$ function have assumed that each channel monomer possessed a single inhibitory Ca^{2+}-binding site, including our previous empirical description of the effects of $InsP_3$ on channel gating (Mak et al., 1998, 2001b). Our previous description assumed a single inhibitory Ca^{2+}binding site whose apparent affinity was allosterically reduced by $InsP_3$ binding. The model derived here now suggests that two Ca^{2+}-binding sites present in each monomer contribute to Ca^{2+} inhibition. Ca^{2+} binding to an $InsP_3$-dependent G site inhibits $InsP_3R$ activity in the absence of $InsP_3$, which is responsible for the lack of channel activity in the absence of $InsP_3$ in normal $[Ca^{2+}]_i$. $InsP_3$ binding to the channel changes the effective affinities of this site, and in so doing transforms it into an activating site. This $InsP_3$-mediated transformation of the nature of this Ca^{2+}-binding site is responsible for all the $InsP_3$-dependence of the channel, accounting for the extremely high sensitivity of Ca^{2+} inhibition of $InsP_3R$ channel gating to small changes in [$InsP_3$]. The second Ca^{2+}-binding site (H site) is strictly inhibitory with a lower Ca^{2+} affinity (10–30 μM) that is not modulated by $InsP_3$ binding. The $InsP_3$ independence of this site is responsible for the lack of further effect of $InsP_3$ on the channel once [$InsP_3$] > 100 nM, accounting for the observation that the effects of $InsP_3$ abruptly saturate around this concentration. Furthermore, Ca^{2+} binding to the H site is responsible for the observed inhibition of the channel even at lower $[Ca^{2+}]_i$ (<10–30 μM), when [$InsP_3$] is <100 nM. Whereas the properties of the H sites are insensitive to $InsP_3$ binding, they are rendered nonfunctional by a nonphysiological protocol: exposure to an ultra-low bath [Ca^{2+}]. Nevertheless, the channel exposed to ultra-low bath [Ca^{2+}] remains dependent on $InsP_3$ because the other Ca^{2+}-binding sites, specifically the $InsP_3$-dependent G site, are not affected by the low bath [Ca^{2+}]. Ca^{2+} binding to the G site inhibits $InsP_3R$ activity in the absence of $InsP_3$.

Our molecular model suggests that not all conformation transitions of the $InsP_3R$ that affect the channel opening are regulated by $InsP_3$ and $[Ca^{2+}]_i$. In our model, P_{max} of the $InsP_3R$ channel is limited to ~0.8 (<1) by conformation transitions that affect channel opening but are independent of $[Ca^{2+}]_i$ and [$InsP_3$]. This can account for the observed constancy of the mean $InsP_3R$ channel open durations over a wide range of $[Ca^{2+}]_i$ and [$InsP_3$]. Such conformation transitions probably arise from a channel gating mechanism different from the one regulated by ligands ($InsP_3$ and Ca^{2+}).

A critical insight that has emerged from analysis of the behavior of the model is that the major effect of $InsP_3$ in regulating the activity of the $InsP_3R$ channel is to tune the nature of the G sites. In contrast, we previously interpreted the effect of $InsP_3$ as tuning the sensitivity of the channel to Ca^{2+} inhibition (Mak et al., 1998, 2001b). How can we reconcile the empirical observation that K_{inh} is tuned by [$InsP_3$] with this insight from the model? Normally, the functional H site has a dissociation constant in the closed B and D conformations of 20–30 μM (Table I). However, the inhibitory effect of the H sites is not only manifested at such high $[Ca^{2+}]_i$. The $[Ca^{2+}]_i$ at which H site-mediated Ca^{2+} inhibition is manifested depends on the properties of the G sites. In low [$InsP_3$] at which the G sites have just become activating, the difference between the effective affinities of the G sites in the closed and active channel

is small so that the extent of G site-mediated activation is limited. On the other hand, there is finite Ca^{2+} binding to the H site even at $[Ca^{2+}]_i << K^{HD}$ (200–300 nM), which strongly stabilizes the closed conformations. This inhibitory effect can be sufficient to counter the activating effect of the F and G sites. Therefore, in the presence of low $[InsP_3]$ with weak G site activation, the H site inhibition is manifested even at low $[Ca^{2+}]_i$. This results in a narrow bell-shape dependence of channel P_o on $[Ca^{2+}]_i$ with the channel achieving a low maximum P_o, as observed (Mak et al., 1998). As $[InsP_3]$ increases, G site activation is enhanced, so Ca^{2+} binding to the G sites stabilizes the active conformations more strongly. The inhibitory effect of H-site binding is then only manifested at higher $[Ca^{2+}]_i$. This generates a wider bell-shape dependence of channel P_o on $[Ca^{2+}]_i$ with the channel exhibiting a higher maximum P_o centered at higher $[Ca^{2+}]_i$.

The maximum channel P_o reaches 0.8 (P_{max}) at $[InsP_3]$ ~30 nM. Further increases in $[InsP_3]$ beyond this cause no further increase in the maximum channel P_o. However, higher $[InsP_3]$ continues to shift the channel equilibria toward the C and D conformations, resulting in stronger G site activation. This delays the onset of observable H site–mediated inhibition to even higher $[Ca^{2+}]_i$, broadening the biphasic dependence of channel P_o on $[Ca^{2+}]_i$ into a plateau shape (Mak et al., 1998). In this manner, $InsP_3$ tuning of the extent of G site activation is empirically manifested as an apparent $InsP_3$-dependent shift in the ability of Ca^{2+} to inhibit the channel.

This model developed here will be useful in guiding future experimental investigations as well as providing insights for understanding existing $InsP_3R$ channel data. First, it will be important for providing a quantitative framework for understanding the roles of other channel regulators. For example, insights into the mechanisms of Mg^{2+} effects on BK channels were greatly facilitated by having available the previously developed complex allosteric schemes that account for Ca^{2+} and voltage regulation of the channel (see Magleby, 2001). In the case of $InsP_3R$, the allosteric model may provide a framework for modeling the effect of ATP, phosphorylation, and other modulators on channel gating. Second, use of the model will be important as mutagenesis is applied to this channel in attempts to discover the molecular bases for ligand regulation. Because effects of mutagenesis may be allosterically coupled to the ligand-binding sites through long-range effects, the model will be important for analyzing mutant channel behavior to discriminate mutations that are truly at the binding sites from those that are allosterically coupled to the binding sites. For example, if a mutation is observed to change the properties of $InsP_3$ activation of channel gating, the target of the mutation could be the $InsP_3$-binding Q site itself, but our model suggests that the mutation could possibly modify the $InsP_3$-dependent, Ca^{2+}-binding G sites instead. With our model, changes in channel behavior resulting from any kind of modulation of the properties of the ligand-binding sites can now be interpreted within the context of the model to make inferences regarding the molecular mechanisms involved, as we have done in our analysis of the effects of ultra-low bath $[Ca^{2+}]$ exposure. For instance, experimental or physiological modulation of the affinity of the G sites in just the C conformation of the channel can affect all the parameters (P_{max}, K_{act}, H_{act}, K_{inh}, H_{inh}) in the empirical Hill equation (Eq. 1). Without a molecular model, it would be extremely difficult to understand the underlying mechanisms just from the effects of the modulation. Indeed, a study of the effects of a point mutation on the gating of the type 1 channel (Tu et al., 2003) was limited to phenomenological description because of a lack of a model by which to quantitatively account for the results. Third, although our model is a general one based on observations made under steady-state conditions, with all the ligand-binding reactions assumed to be possible in any sequential order, it can nevertheless incorporate sequential binding models in which certain ligand binding sequences are "forbidden", like that proposed in (Marchant and Taylor, 1997; Adkins and Taylor, 1999) in which Ca^{2+} cannot bind to the activating sites before $InsP_3$ binds to the $InsP_3$-binding sites. Our model can incorporate sequential schemes because it only explicitly involves the equilibrium constants of ligand binding and conformation transitions. Thus, "forbidden" ligand binding sequences can be incorporated simply by assuming that certain ligand binding and conformation transitions have much slower reaction rates than other reactions in the ligand binding scheme. The model may also be useful in predicting which transitions are "forbidden". Fourth, when transient kinetic responses of channels are measured in response to ligand concentration changes, our model with its specified equilibrium constants may help to constrain the set of possible schemes and values of reaction rate constants that need to be considered. Fifth, application of the model to datasets obtained from various $InsP_3R$ isoforms may prove useful in identifying the properties that distinguish them and account for any observed distinct behaviors. For example, the type 2 $InsP_3R$ channel was reported to be distinct from the type 1 channel in its relative lack of high Ca^{2+} inhibition (Ramos-Franco et al., 2000). Our model suggests that this difference could be accounted for by a less effective inhibitory H site in the type 2 channel.

Finally, besides its application to enhance our understanding of the regulation of $InsP_3R$ channel gating, the modeling effort described here has extended sub-

stantially the basic MWC model upon which it is based. Our systematic mathematical treatment of not only the MWC-based four-plus-two-conformation model, but also of the other MWC-based and non-MWC models (presented in the online supplemental material section) may be useful in future modeling of other allosteric processes involving multiple ligands.

APPENDIX

MWC-based Four-Plus-Two-Conformation Model—Model e

In this allosteric model, the homotetrameric $InsP_3R$ channel can assume six conformations: four (A*, B, C*, and D) that are connected by ligand dependent transitions, plus two (A′ and C′) that are connected to the others by ligand independent transitions (hence the name). The channel is open in two conformations (A* and C*), and closed in the others (B, D, A′ and C′). However, since the transitions A*↔A′ and C*↔C′ are ligand independent, we consider the conformations A* and A′ as one active conformation A; and C* and C′ as one active conformation C when we examine the regulation of $InsP_3R$ channel activity by ligands $InsP_3$ and Ca^{2+} (Fig. 7).

Each $InsP_3R$ monomer has three Ca^{2+}-binding sites (F, G, and H) and one $InsP_3$-binding site (Q). The ligand-binding status of an $InsP_3R$ tetrameric channel can be represented using the convention in which ${}^{h}_{q}A^{g}_{f}$ represents the channel in the A conformation with f Ca^{2+} bound to the F sites, g Ca^{2+} bound to the G sites, h Ca^{2+} bound to the H sites, and q $InsP_3$ molecules bound to the Q sites ($0 \le f, g, h, q \le 4$).

Based on the simplifications assumed in the MWC model (Monod et al., 1965), all the F sites in an $InsP_3R$ channel in conformation A have the same dissociation constant for Ca^{2+} binding (represented as K^{FA} in this discussion), regardless of the ligand-binding status of the channel. Other dissociation constants are represented similarly, like K^{GA} and K^{QC}. After the derivation in Monod et al. (1965), these dissociation constants (a total of 16 for 4 sites in 4 conformations) together with the three independent equilibrium constants (L_{BA}, L_{CA}, and L_{DB}) for conformation transitions between unliganded channels (${}^{0}_{0}A^{0}_{0} \leftrightarrow {}^{0}_{0}B^{0}_{0}$, ${}^{0}_{0}A^{0}_{0} \leftrightarrow {}^{0}_{0}C^{0}_{0}$, and ${}^{0}_{0}B^{0}_{0} \leftrightarrow {}^{0}_{0}D^{0}_{0}$ respectively) constitute the full set of parameters that completely describes the regulation by $InsP_3$ and Ca^{2+} of the conformation changes of the $InsP_3R$ channel. Using the symbol conventions described above, the concentration of the $InsP_3R$ channel in any specific ligand-binding state, $[{}^{h}_{q}A^{g}_{f}]$, can be expressed in terms of $[InsP_3]$, $[Ca^{2+}]_i$, $[{}^{0}_{0}A^{0}_{0}]$, and the set of parameters:

$$[{}^{h}_{q}A^{g}_{f}] = \frac{4!}{f!(4-f)!}\left(\frac{[Ca^{2+}]_i}{K^{FA}}\right)^{f}\frac{4!}{g!(4-g)!}\left(\frac{[Ca^{2+}]_i}{K^{GA}}\right)^{g} \frac{4!}{h!(4-h)!}\left(\frac{[Ca^{2+}]_i}{K^{HA}}\right)^{h}\frac{4!}{q!(4-q)!}\left(\frac{[InsP_3]}{K^{QA}}\right)^{q}[{}^{0}_{0}A^{0}_{0}] \quad (5)$$

Similar equations can be derived to express ligand-binding states of other conformations.

For our model of ligand regulation of $InsP_3R$ gating, we postulate that $[Ca^{2+}]_i$ mainly regulates the equilibrium A↔B and C↔D. Furthermore, we postulate that F is an activating Ca^{2+}-binding site, whereas H is an inhibitory Ca^{2+}-binding site. This means that K^{FA} and $K^{FC} < K^{FB}$ and K^{FD}, so that Ca^{2+} binding to the activating F sites stabilizes the active conformations. In contrast, K^{HA} and $K^{HC} > K^{HB}$ and K^{HD}, so that Ca^{2+} binding to the inhibitory H sites stabilizes the closed conformations.

On the other hand, $[InsP_3]$ regulates the A↔C and B↔D equilibria, modulating channel P_o by stabilizing the C and D channel conformations relative to the A and B conformations (K^{QA} and $K^{QB} >> K^{QC}$ and K^{QD}).

The observed independence of the Ca^{2+} activation of the channel on $[InsP_3]$ (condition ii) constrains the number of free parameters involved in this model. Because $K^{FA} \neq K^{FB}$ and $K^{FC} \neq K^{FD}$, the $InsP_3$ affinity of the Q sites must be the same for the A and B conformations ($K^{QA} = K^{QB}$), and for the C and D conformations ($K^{QC} = K^{QD}$) so that $InsP_3$ binding to the channel does not affect the equilibria A↔B and C↔D. This prevents $InsP_3$ binding to the channel from shifting the equilibria A↔B, or C↔D, thus leaving Ca^{2+} activation of the channel unaffected by $[InsP_3]$. To emphasize this constraint, we define $K^{Q1} = K^{QA} = K^{QB}$, and $K^{Q2} = K^{QC} = K^{QD}$. Furthermore, because $InsP_3$ binding to the Q sites does affect the equilibria A↔C and B↔D (that is how $InsP_3$ regulates the channel), the affinity of the F sites must be the same in the A and C conformations ($K^{FA} = K^{FC}$) and the same in the B and D conformations ($K^{FB} = K^{FD}$), so that shifts in the equilibria A↔C and B↔D due to $InsP_3$ binding will not affect Ca^{2+} activation either. Again, to emphasize the constraint on these dissociation constants, we define $K^{F1} = K^{FA} = K^{FC}$ and $K^{F2} = K^{FB} = K^{FD}$.

Even though Ca^{2+} inhibition of $InsP_3R$ is very sensitive to change in $[InsP_3]$ from 10 to 100 nM, Ca^{2+} inhibition does not change any more once $[InsP_3]$ reaches 100 nM despite a further three orders of magnitude increase in $[InsP_3]$ (from 100 nM to 180 μM). Thus, higher $[InsP_3]$ beyond 100 nM does not require higher $[Ca^{2+}]_i$ for inhibition (condition v). This indicates that Ca^{2+} binding to the H sites is not affected by $[InsP_3]$. Therefore, much like the relation between the dissociation constants of the F sites ($K^{FA} = K^{FC} = K^{F1}$ and $K^{FB} = K^{FD} = K^{F2}$), the dissociation constants of the H sites in the A and C channel conformations are the same ($K^{HA} = K^{HC} = K^{H1}$), and those in the B and D conformations are the same ($K^{HB} = K^{HD} = K^{H2}$).

The concentrations of the $InsP_3R$ channel in one conformation regardless of its ligand-binding status is shown in Eq. 6.

$$\left.\begin{aligned}
[\mathrm{A}] &= \sum_{f,g,h,q=0}^{4} [{}_{q}^{h}\mathrm{A}_{f}^{g}] = [{}_{0}^{0}\mathrm{A}_{0}^{0}](1+[\mathrm{Ca}^{2+}]_i/K^{\mathrm{F1}})^4(1+[\mathrm{Ca}^{2+}]_i/K^{\mathrm{GA}})^4(1+[\mathrm{Ca}^{2+}]_i/K^{\mathrm{H1}})^4(1+[\mathrm{InsP_3}]/K^{\mathrm{Q1}})^4\\
[\mathrm{B}] &= L_{\mathrm{BA}}[{}_{0}^{0}\mathrm{A}_{0}^{0}](1+[\mathrm{Ca}^{2+}]_i/K^{\mathrm{F2}})^4(1+[\mathrm{Ca}^{2+}]_i/K^{\mathrm{GB}})^4(1+[\mathrm{Ca}^{2+}]_i/K^{\mathrm{H2}})^4(1+[\mathrm{InsP_3}]/K^{\mathrm{Q1}})^4\\
[\mathrm{C}] &= L_{\mathrm{CA}}[{}_{0}^{0}\mathrm{A}_{0}^{0}](1+[\mathrm{Ca}^{2+}]_i/K^{\mathrm{F1}})^4(1+[\mathrm{Ca}^{2+}]_i/K^{\mathrm{GC}})^4(1+[\mathrm{Ca}^{2+}]_i/K^{\mathrm{H1}})^4(1+[\mathrm{InsP_3}]/K^{\mathrm{Q2}})^4\\
[\mathrm{D}] &= L_{\mathrm{BA}}L_{\mathrm{DB}}[{}_{0}^{0}\mathrm{A}_{0}^{0}](1+[\mathrm{Ca}^{2+}]_i/K^{\mathrm{F2}})^4(1+[\mathrm{Ca}^{2+}]_i/K^{\mathrm{GD}})^4(1+[\mathrm{Ca}^{2+}]_i/K^{\mathrm{H2}})^4(1+[\mathrm{InsP_3}]/K^{\mathrm{Q2}})^4
\end{aligned}\right\} \quad (6)$$

The open probability P_o of a single $InsP_3R$ channel is the fraction of time the channel spends in the open A* and C* conformations. In a stationary system, this is the same as the relative abundance of channels that adopt the open conformations in an ensemble of many (ideally infinite) channels, i.e.,

$$P_o = ([\mathrm{A}^*]+[\mathrm{C}^*])/([\mathrm{A}]+[\mathrm{B}]+[\mathrm{C}]+[\mathrm{D}]). \quad (7)$$

Whereas the equilibria between the B, D, A*, and C* conformations are ligand dependent, the equilibrium constants R_A and R_C for the transitions A*↔A′ and C*↔C′, respectively, are independent of $[InsP_3]$ and $[Ca^{2+}]_i$. Because the experimental parameter P_{max} is not affected by $[InsP_3]$ (Mak et al., 1998, 2001b), $R_A = R_C = R$. Thus,

$$\left.\begin{aligned}
[\mathrm{A}^*] &= [\mathrm{A}][R/(1+R)]\\
[\mathrm{C}^*] &= [\mathrm{C}][R/(1+R)]
\end{aligned}\right\} \quad (8)$$

This means that the channel is open for only a fraction $[R/(1 + R)]$ of the time it is in the A or C conformation. This allows the model an extra degree of freedom to fit the experimentally observed channel P_{max}, found to be <1 (condition ix). Together, Eqs. 6–8 describe the channel P_o under all $[Ca^{2+}]_i$ and $[InsP_3]$ with 14 free parameters (Table I).

We would like to thank Dr. F.T. Horrigan (University of Pennsylvania) and Dr. S. Ponce-Dawson (University of Buenos Aires, Argentina) for reviewing our manuscript before submission and giving us many helpful comments.

This work was supported by grants to J.K. Foskett from the NIH (MH59937, GM56328) and to D.-O.D. Mak from the American Heart Association (9906220U).

Olaf S. Andersen served as editor.

Submitted: 24 July 2003
Accepted: 16 September 2003

REFERENCES

Adkins, C.E., and C.W. Taylor. 1999. Lateral inhibition of inositol 1,4,5-trisphosphate receptors by cytosolic Ca^{2+}. *Curr. Biol.* 9:1115–1118.

Baudet, S.B., L. Hove-Madsen, and D.M. Bers. 1994. How to make and use calcium-specific mini- and microelectrodes. *In* A Practical Guide to the Study of Calcium in Living Cells. 1st ed. R. Nuccitelli, editor. Academic Press, San Diego. 94–114.

Berridge, M.J. 1993. Inositol trisphosphate and calcium signalling. *Nature.* 361:315–325.

Bezprozvanny, I., J. Watras, and B.E. Ehrlich. 1991. Bell-shaped calcium-response curves of $Ins(1,4,5)P_3$- and calcium-gated channels from endoplasmic reticulum of cerebellum. *Nature.* 351: 751–754.

Boehning, D., S.K. Joseph, D.-O.D. Mak, and J.K. Foskett. 2001. Single-channel recordings of recombinant inositol trisphosphate receptors in mammalian nuclear envelope. *Biophys. J.* 81:117–124.

Changeux, J.P., and S.J. Edelstein. 1998. Allosteric receptors after 30 years. *Neuron.* 21:959–980.

Cullen, P.J., J.G. Comerford, and A.P. Dawson. 1988. Heparin inhibits the inositol 1,4,5-trisphosphate-induced Ca^{2+} release from rat liver microsomes. *FEBS Lett.* 228:57–59.

De Young, G.W., and J. Keizer. 1992. A single-pool inositol 1,4,5-trisphosphate-receptor-based model for agonist-stimulated oscillations in Ca^{2+} concentration. *Proc. Natl. Acad. Sci. USA.* 89:9895–9899.

Iino, M. 1990. Biphasic Ca^{2+} dependence of inositol 1,4,5-trisphosphate-induced Ca^{2+} release in smooth muscle cells of the guinea pig taenia caeci. *J. Gen. Physiol.* 95:1103–1122.

Jackson, M.B. 1984. Spontaneous openings of the acetylcholine receptor channel. *Proc. Natl. Acad. Sci. USA.* 81:3901–3904.

Jiang, Q., D.-O.D. Mak, S. Devidas, E.M. Schwiebert, A. Bragin, Y. Zhang, W.R. Skach, W.B. Guggino, J.K. Foskett, and J.F. Engelhardt. 1998. Cystic fibrosis transmembrane conductance regulator-associated ATP release is controlled by a chloride sensor. *J. Cell Biol.* 143:645–657.

Jones, S.W. 1999. Commentary: a plausible model. *J. Gen. Physiol.* 114:271–275.

Joseph, S.K., C. Lin, S. Pierson, A.P. Thomas, and A.R. Maranto. 1995. Heteroligomers of type-I and type-III inositol trisphosphate receptors in WB rat liver epithelial cells. *J. Biol. Chem.* 270:23310–23316.

Kaftan, E.J., B.E. Ehrlich, and J. Watras. 1997. Inositol 1,4,5-trisphosphate ($InsP_3$) and calcium interact to increase the dynamic range of $InsP_3$ receptor-dependent calcium signaling. *J. Gen. Physiol.* 110:529–538.

Liu, D.T., G.R. Tibbs, P. Paoletti, and S.A. Siegelbaum. 1998. Constraining ligand-binding site stoichiometry suggests that a cyclic nucleotide-gated channel is composed of two functional dimers. *Neuron.* 21:235–248.

Magleby, K.L. 2001. Kinetic gating mechanisms for BK channels: when complexity leads to simplicity. *J. Gen. Physiol.* 118:583–587.

Mak, D.-O.D., and J.K. Foskett. 1994. Single-channel inositol 1,4,5-trisphosphate receptor currents revealed by patch clamp of isolated Xenopus oocyte nuclei. *J. Biol. Chem.* 269:29375–29378.

Mak, D.-O.D., and J.K. Foskett. 1997. Single-channel kinetics, inactivation, and spatial distribution of inositol trisphosphate (IP_3) receptors in Xenopus oocyte nucleus. *J. Gen. Physiol.* 109:571–587.

Mak, D.-O.D., and J.K. Foskett. 1998. Effects of divalent cations on single-channel conduction properties of Xenopus IP_3 receptor. *Am. J. Physiol.* 275:C179–C188.

Mak, D.-O.D., S. McBride, and J.K. Foskett. 1998. Inositol 1,4,5-trisphosphate activation of inositol trisphosphate receptor Ca^{2+} channel by ligand tuning of Ca^{2+} inhibition. *Proc. Natl. Acad. Sci. USA.* 95:15821–15825.

Mak, D.-O.D., S. McBride, and J.K. Foskett. 1999. ATP regulation of type 1 inositol 1,4,5-trisphosphate receptor channel gating by allosteric tuning of Ca^{2+} activation. *J. Biol. Chem.* 274:22231–22237.

Mak, D.-O.D., S. McBride, V. Raghuram, Y. Yue, S.K. Joseph, and J.K. Foskett. 2000. Single-channel properties in endoplasmic reticulum membrane of recombinant type 3 inositol trisphosphate receptor. *J. Gen. Physiol.* 115:241–256.

Mak, D.-O.D., S. McBride, and J.K. Foskett. 2001a. ATP regulation of recombinant type 3 inositol 1,4,5-trisphosphate receptor gating. *J. Gen. Physiol.* 117:447–456.

Mak, D.-O.D., S. McBride, and J.K. Foskett. 2001b. Regulation by Ca^{2+} and inositol 1,4,5-trisphosphate ($InsP_3$) of single recombinant type 3 $InsP_3$ receptor channels. Ca^{2+} activation uniquely distinguishes types 1 and 3 $InsP_3$ receptors. *J. Gen. Physiol.* 117:435–446.

Mak, D.-O.D., S. McBride, and J.K. Foskett. 2001c. ATP-dependent adenophostin activation of inositol 1,4,5-trisphosphate receptor channel gating: kinetic implications for the durations of calcium puffs in cells. *J. Gen. Physiol.* 117:299–314.

Mak, D.-O.D., S. McBride, N.B. Petrenko, and J.K. Foskett. 2003. Novel regulation of calcium inhibition of the inositol 1,4,5-trisphosphate receptor calcium-release channel. *J. Gen. Physiol.* 122: 583–603.

Marchant, J.S., M.D. Beecroft, A.M. Riley, D.J. Jenkins, R.D. Marwood, C.W. Taylor, and B.V. Potter. 1997. Disaccharide polyphosphates based upon adenophostin A activate hepatic D-myo-inositol 1,4,5-trisphosphate receptors. *Biochemistry.* 36:12780–12790.

Marchant, J.S., and C.W. Taylor. 1997. Cooperative activation of IP_3 receptors by sequential binding of IP_3 and Ca^{2+} safeguards against spontaneous activity. *Curr. Biol.* 7:510–518.

Meyer, T., D. Holowka, and L. Stryer. 1988. Highly cooperative opening of calcium channels by inositol 1,4,5-trisphosphate. *Science.* 240:653–655.

Meyer, T., and L. Stryer. 1991. Calcium spiking. *Annu. Rev. Biophys. Biophys. Chem.* 20:153–174.

Mikoshiba, K., T. Furuichi, A. Miyawaki, S. Yoshikawa, T. Nakagawa, N. Yamada, Y. Hamanaka, I. Fujino, T. Michikawa, Y. Ryo, et al. 1993. Inositol trisphosphate receptor and Ca^{2+} signalling. *Philos. Trans. R. Soc. Lond. B Biol. Sci.* 340:345–349.

Monod, J., J. Wyman, and J.-P. Changeux. 1965. On the nature of allosteric transitions: a plausible model. *J. Mol. Biol.* 12:88–118.

Moraru, I.I., E.J. Kaftan, B.E. Ehrlich, and J. Watras. 1999. Regulation of type 1 inositol 1,4,5-trisphosphate-gated calcium channels by $InsP_3$ and calcium - Simulation of single channel kinetics based on ligand binding and electrophysiological analysis. *J. Gen. Physiol.* 113:837–849.

Patel, S., S.K. Joseph, and A.P. Thomas. 1999. Molecular properties of inositol 1,4,5-trisphosphate receptors. *Cell Calcium.* 25:247–264.

Picones, A., and J.I. Korenbrot. 1995. Spontaneous, ligand-independent activity of the cGMP-gated ion channels in cone photoreceptors of fish. *J. Physiol.* 485:699–714.

Ramos-Franco, J., D. Bare, S. Caenepeel, A. Nani, M. Fill, and G. Mignery. 2000. Single-channel function of recombinant type 2 inositol 1,4, 5- trisphosphate receptor. *Biophys. J.* 79:1388–1399.

Richards, M.J., and S.E. Gordon. 2000. Cooperativity and cooperation in cyclic nucleotide-gated ion channels. *Biochemistry.* 39: 14003–14011.

Sienaert, I., H. De Smedt, J.B. Parys, L. Missiaen, S. Vanlingen, H. Sipma, and R. Casteels. 1996. Characterization of a cytosolic and a luminal Ca^{2+} binding site in the type I inositol 1,4,5-trisphosphate receptor. *J. Biol. Chem.* 271:27005–27012.

Sienaert, I., L. Missiaen, H. De Smedt, J.B. Parys, H. Sipma, and R. Casteels. 1997. Molecular and functional evidence for multiple Ca^{2+}-binding domains in the type 1 inositol 1,4,5-trisphosphate receptor. *J. Biol. Chem.* 272:25899–25906.

Swillens, S., L. Combettes, and P. Champeil. 1994. Transient inositol 1,4,5-trisphosphate-induced Ca^{2+} release: A model based on regulatory Ca^{2+}-binding sites along the permeation pathway. *Proc. Natl. Acad. Sci. USA.* 91:10074–10078.

Swillens, S., P. Champeil, L. Combettes, and G. Dupont. 1998. Stochastic simulation of a single inositol 1,4,5-trisphosphate-sensitive Ca^{2+} channel reveals repetitive openings during 'blip-like' Ca^{2+} transients. *Cell Calcium.* 23:291–302.

Takahashi, M., K. Tanzawa, and S. Takahashi. 1994. Adenophostins, newly discovered metabolites of *Penicillium brevicompactum*, act as potent agonists of the inositol 1,4,5-trisphosphate receptor. *J. Biol. Chem.* 269:369–372.

Toescu, E.C. 1995. Temporal and spatial heterogeneities of Ca^{2+} signaling: Mechanisms and physiological roles. *Am. J. Physiol.* 269:G173–G185.

Tu, H., E. Nosyreva, T. Miyakawa, Z. Wang, A. Mizushima, M. Iino, and I. Bezprozvanny. 2003. Functional and biochemical analysis of the type 1 inositol (1,4,5)-trisphosphate receptor calcium sensor. *Biophys. J.* 85:290–299.

Worley, P.F., J.M. Baraban, S. Supattapone, V.S. Wilson, and S.H. Snyder. 1987. Characterization of inositol trisphosphate receptor binding in brain. Regulation by pH and calcium. *J. Biol. Chem.* 262:12132–12136.

Yang, J., S. McBride, D.O. Mak, N. Vardi, K. Palczewski, F. Haeseleer, and J.K. Foskett. 2002. Identification of a family of calcium sensors as protein ligands of inositol trisphosphate receptor Ca^{2+} release channels. *Proc. Natl. Acad. Sci. USA.* 99:7711–7716.

Yoshikawa, F., M. Morita, T. Monkawa, T. Michikawa, T. Furuichi, and K. Mikoshiba. 1996. Mutational analysis of the ligand binding site of the inositol 1,4,5- trisphosphate receptor. *J. Biol. Chem.* 271:18277–18284.